



BRNO UNIVERSITY OF TECHNOLOGY

VYSOKÉ UČENÍ TECHNICKÉ V BRNĚ

FACULTY OF CHEMISTRY

FAKULTA CHEMICKÁ

INSTITUTE OF MATERIALS SCIENCE

ÚSTAV CHEMIE MATERIÁLŮ

RHEOLOGICAL PROPERTIES OF MODIFIED POLYMER-COMPOSITE BONE PASTES

REOLOGICKÉ VLASTNOSTI MODIFIKOVANÝCH POLYMER-
KOMPOZITNÍCH KOSTNÍCH PAST

MASTER'S THESIS

DIPLOMOVÁ PRÁCE

AUTHOR

AUTOR PRÁCE

Bc. Kristýna Valová

SUPERVISOR

VEDOUCÍ PRÁCE

Ing. Lenka Michlovská, Ph.D.

BRNO 2018

Zadání diplomové práce

Číslo práce: FCH-DIP1197/2017
Ústav: Ústav chemie materiálů
Studentka: **Bc. Kristýna Valová**
Studijní program: Chemie, technologie a vlastnosti materiálů
Studijní obor: Chemie, technologie a vlastnosti materiálů
Vedoucí práce: **Ing. Lenka Michlovská, Ph.D.**
Akademický rok: 2017/18

Název diplomové práce:

Reologické vlastnosti modifikovaných polymer–kompozitních kostních past

Zadání diplomové práce:

- 1) Lit. rešerše na téma fosfátové cementy a jejich aditiva se zaměřením na reologii
- 2) Optimalizace nastavení a parametrů pro reologické měření kompozitních cementů
- 3) Stanovení viskoelastických vlastností modifikovaných cementů
- 4) Vyhodnocení a diskuze
- 5) Závěr

Termín odevzdání diplomové práce: 7.5.2018

Diplomová práce se odevzdává v děkanem stanoveném počtu exemplářů na sekretariát ústavu. Toto zadání je součástí diplomové práce.

Bc. Kristýna Valová
student(ka)

Ing. Lenka Michlovská, Ph.D.
vedoucí práce

prof. RNDr. Josef Jančář, CSc.
vedoucí ústavu

V Brně dne 31.1.2018

prof. Ing. Martin Weiter, Ph.D.
děkan

ABSTRACT

Diploma thesis is focused on study of visco-elastic behavior of bone pastes based on calcium phosphate and the aqueous solution of biodegradable termosensitive triblock copolymer improving flowing properties of the paste. In the theoretical part, a brief characterization of calcium phosphate cements is elaborated. It also deals with the characteristics of rheological properties of injectable bone pastes. It includes a brief overview of additives influencing the rheological and mechanical properties of pastes. The experimental part was firstly focused on the triblock copolymer characterization by proton nuclear magnetic resonance spectroscopy and rheology. Secondly, the preparation of modified polymer-phosphate pastes was evaluated in terms of visco-elastic properties. Bone paste was modified by the addition of adhesive compounds (dopamine and sodium iodate) and antibacterial compound (selenium nanoparticles). Visco-elastic properties were performed by rheological analysis, during which the setting process proceeded exhibiting significant changes in the thixotropic behavior of both unmodified and modified phosphate pastes. The setting process took place at 23 °C and 37 °C imiting physiological environment. Morphology of polymer-phosphate pastes was characterized by scanning electron microscopy and the particle size was determined using a laser particle analyzer.

It has been shown that the above-mentioned additives had a positive effect on the kinetics of self-setting paste process, moreover, selenium nanoparticles improved as well thixotropic behaviors of polymer-phosphate pastes. Therefore, novel injectable composite bone pastes are suitable for mini-invasive surgery in terms of treating fractures due to the adhesion additives as well as for osteomyelitis treatment due to the possible release of antibacterial nanoparticles.

KEY WORDS

Calcium phosphate cement, injectable bone paste, biodegradable polymer, dopamine, rheological properties, thixotropy.

ABSTRAKT

Předložená diplomová práce je zaměřená na studium viscoelastického chování kostních past na bázi fosforečnanu vápenatého a vodného roztoku termosenzitivního triblokového kopolymeru, zlepšujícího tokové vlastnosti pasty. V teoretické části je zpracována stručná charakteristika cementů na bázi fosforečnanu vápenatého. Rovněž se zabývá charakteristikou reologických vlastností injektabilních kostních past. Součástí je také stručný přehled aditiv ovlivňujících právě reologické a mechanické vlastnosti past. Experimentální část je zaměřena na charakterizaci triblokového kopolymeru pomocí nukleární magnetické rezonanční spektroskopie a reologie. Dále byly připravovány modifikované fosfátové cementy, u kterých byly posléze studovány viskoelastické vlastnosti. Kostní pasta byla modifikována přidavkem adhezivních sloučenin (dopamin a jodičnan sodný) a antibakteriálním činidlem (selenové nanočástice). Analýza viskoelastických vlastností byla provedena reologickou analýzou, během níž byl primárně sledován proces vytvrzování a tixotropní chování jak nemodifikovaných, tak modifikovaných fosfátových past. Proces vytvrzování probíhal při teplotě 23 °C a 37 °C, imitující fyziologické prostředí. Morfologie fosfátové keramiky byla charakterizována pomocí rastrovací elektronové mikroskopie a velikost částic byla zjištěna pomocí laserového analyzátoru částic.

Bylo prokázáno, že výše zmíněná aditiva mají pozitivní vliv na kinetiku procesu vytvrzování kostních past. Selenové nanočástice navíc vylepšily tixotropní chování polymer-fosfátových past. Z tohoto důvodu jsou tyto nové injektabilní kompozitní pasty vhodné pro miniinvazivní chirurgii. Díky aditivům, vykazujících adhezivní vlastnosti, mají potenciál uplatnit se při léčbě zlomenin. Stejně tak se nabízí možnost využít pasty při léčbě osteomyelitidy, a to díky možnému uvolňování antibakteriálních nanočástic.

KLÍČOVÁ SLOVA

Fosfátové cementy, injektabilní kostní pasta, biodegradabilní polymer, dopamin, reologické vlastnosti, tixotropie.

VALOVÁ, K. *Rheological properties of modified polymer-composite bone pastes*. Brno: Brno University of Technology, Faculty of Chemistry, 2018. 66 p. Supervisor Ing. Lenka Michlovská, Ph.D..

DECLARATION

I declare that the diploma thesis has been worked out by myself and that all the quotations from the used literary sources are accurate and complete. The content of the diploma thesis is the property of the Faculty of Chemistry of Brno University of Technology and all commercial uses are allowed only if approved by both the supervisor and the dean of the Faculty of Chemistry, BUT.

.....

student's signature

Acknowledgement

I would like to thank my supervisor Lenka Michlovská, PhD. for valuable advice, helpfulness, patience and time which she has gave to me. I would also like to thank Assoc. Prof. Lucy Vojtová for valuable advice. I also thank to Petr Poláček, PhD. and Ivana Chamradová, PhD. for helping and explaining rheological measurements, Assoc. Prof Klára Částková for the measurement of particle size distribution, Dr. Otakar Humpa for NMR measurement and Bc. Simona Debnárová for copolymer synthesis. I would like to thank my colleagues from the laboratory for their willingness and help. Last but not least I would like to express my thanks to my dear family and boyfriend for their support not only during the study.

This work was supported by the CEITEC 2020 (LQ1601) with financial support from the Ministry of Education, Youth and Sports of the Czech Republic under the National Sustainability Programme II.

TABLE OF CONTENT

1	INTRODUCTION.....	8
2	THEORETICAL PART	9
2.1	Bone.....	9
2.1.1	Bone Renewal	9
2.1.2	Bone Defects Treatment Possibilities	10
2.1.2.1	Bone Grafts	10
2.1.2.2	Bone Tissue Engineering	10
2.2	Calcium Phosphate Cement.....	11
2.2.1	Types of CPC	12
2.2.2	Powder Phase of CPC	13
2.2.3	Liquid Phase of CPC	14
2.2.3.1	Temperature Responsive Triblock Copolymer	15
2.2.4	Additives for CPC	16
2.2.4.1	Dopamine	17
2.2.4.2	Selenium Nanoparticles	19
2.2.5	Biomedical Application of CPC.....	20
2.2.6	Commercially Available CPC	20
2.3	Rheology.....	22
2.3.1	Newtonian Fluid.....	22
2.3.2	Non-Newtonian Fluid.....	23
2.4	Rheology of CPC.....	24
2.4.1	Viscoelastic Behaviour Measurement of CPC	25
2.4.1.1	Dynamic Oscillatory Testing	26
2.4.1.2	Steady State Testing.....	28
3	MAIN GOALS OF THE WORK.....	30
4	EXPERIMENTAL PART	31
4.1	Chemicals	31
4.2	Equipments	31
4.3	Methods	31
4.3.1	Synthesis and Purification of PLGA-PEG-PLGA Copolymer	31
4.3.2	Preparation of PLGA-PEG-PLGA Copolymer Solution	32

4.3.3	Preparation of PLGA-PEG-PLGA/CP Composites	32
4.3.4	Preparation of PLGA-PEG-PLGA/DOPA/CP Composites	32
4.3.5	Preparation of PLGA-PEG-PLGA/DOPA/NaIO ₃ /CP Composites.....	33
4.4	Characterization.....	33
4.4.1	Proton Nuclear Magnetic Resonance Spectroscopy.....	33
4.4.2	Laser Particle Sizer Analyzer	33
4.4.3	Dynamic Light Scattering	33
4.4.4	Scanning Electron Microscopy	33
4.4.5	Dynamic Rheological Analyses	33
4.4.5.1	CPC Rheological Analyses	33
4.4.5.2	PLGA-PEG-PLGA Rheological Analyses	34
4.4.6	Steady State Rheological Analyses	34
5	RESULTS AND DISCUSSION.....	35
5.1	PLGA-PEG-PLGA Triblock Copolymer Analysis	35
5.1.1	Characterization by NMR Spectroscopy.....	35
5.1.2	Rheological Properties Characterization.....	36
5.2	Calcium Phosphate Powder Analysis	37
5.3	Selenium Nanoparticles Analysis	38
5.4	Rheological Behavior of Modified PLGA-PEG-PLGA/CP Pastes.....	39
5.4.1	Measurement Optimization	40
5.4.2	Steady Rheological Properties of Modified CPC.....	40
5.4.3	Linear Viscoelastic Region	45
5.4.3.1	Strain Sweep	45
5.4.3.2	Frequency Sweep	46
5.4.4	Time Sweep Response	47
6	CONCLUSION.....	52
7	REFERENCES.....	53
8	LIST OF TABLES	60
9	LIST OF FIGURES	61
10	LIST OF ABBREVIATIONS.....	64
11	LIST OF SYMBOLS.....	66

1 INTRODUCTION

Calcium phosphate bone cement (CPC) has been a subject of interest in bone tissue engineering for over 30 years. It is hydraulic cement composed of calcium orthophosphate, which forms a moldable paste after mixing with the liquid phase. The paste is capable of self-setting in vivo at physiological conditions (ionic and enzymatic environment, 100% humidity and 37 °C). One of the main positive of CPC is its injectability, which predisposes the cement to application via mini-invasive surgical procedures. For this reason, they have a great potential in the field of orthopedics, traumatology (fracture fixation) or dentistry. Each of these applications needs different requirements in particular for biomechanics. The advantage of CPC is the ability to tailor its properties (rheological, structural, mechanical or bioactive) to meet specific application.

In order of mini-invasive surgery application, the bone pastes need to exhibit the best rheological properties such as injectability, cohesion, or setting time. There are several ways to reach these features. One way is to modify the CPC by the additive that affects the above mentioned properties. Due to the nature of possible CPC applications, the properties of the materials from which they are made are highly demanding. Essential requirements include, in particular, zero toxicity, biodegradability and biocompatibility. A very attractive additive for these purposes appears to be the amino acid dopamine. A mussel-inspired dopamine is polymerizing in an aqueous environment and exhibits excellent adhesion to most surfaces. Up to now dopamine (respectively polydopamine) has been investigated as a coating of different biomaterials. However, it is novel additive for CPC preparation and a challenge in the field of this dynamically developing field of tissue engineering.

This work aims to evaluate rheological properties of the CPC based on alpha tricalcium phosphate, monocalcium phosphate and aqueous solution of PLGA-PEG-PLGA triblock copolymer modified with dopamine, sodium iodate and selenium nanoparticles. Primarily, the thixotropic behaviors of CPC have been studied affecting the CPC injectability. The goal of the work was also an observation of the CPC setting process kinetics using a rotary rheometer. Rheological analysis is one of the most appropriate methods for assessing whether modified CPC can be used as injectable bone pastes for biomedical applications.

2 THEORETICAL PART

2.1 Bone

Bone is a highly specialized, complexed and mineralized connective tissue, which provides wide range of functions in body like: skeletal and locomotion support, internal organ protection, storage of calcium and phosphate ions for homeostasis and elements for hematopoiesis. Skeletal system is composed of more than 200 bones differing in structural and mechanical properties. We distinguish two types of bone, lamellar (Harvesian) bone and fibrillar bone. Fibrillar bone occurs rarer (i.e., dental cement). Lamellar bone may be divided into compact (cortical) and trabecular (spongy) bone which are formed by alternation with the bone cells layer and calcified extracellular matrix as Fig. 1 describes. Extracellular matrix (ECM) is composed of both organic and inorganic phase. The organic phase of matrix is formed by collagenous fibers type I (95 %), proteoglycans and several non-collagenous proteins (5 %). The organic matrix, which is calcified by calcium phosphate minerals, contains bone cells (osteoprogenitor cells, osteoblasts, osteoclast, and osteocytes) that are responsible to the bone organization (i.e., bone renewal) [1, 2, 3].

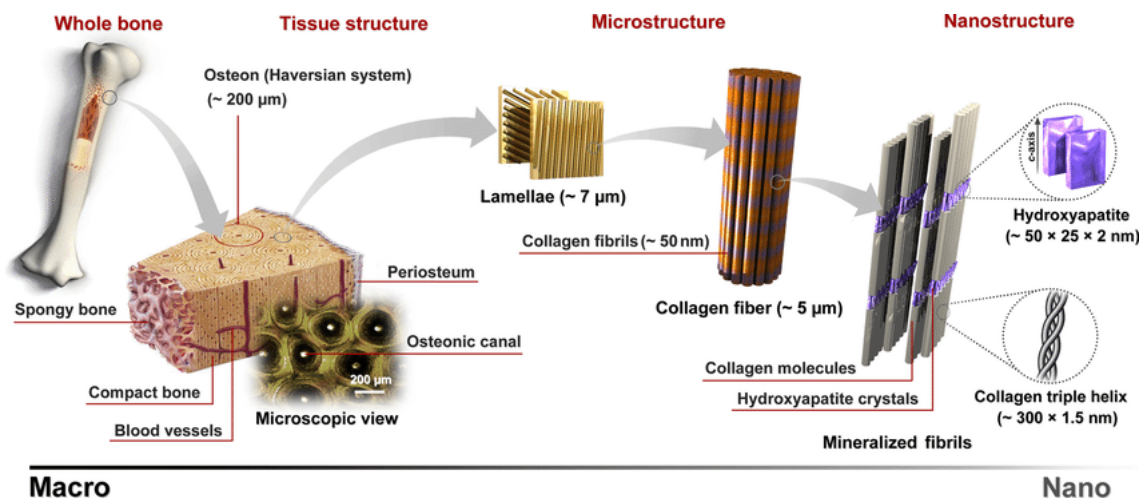


Fig. 1: The hierarchical structure of lamellar bone from macro to nano scale [4].

2.1.1 Bone Renewal

Throughout life, bones dispose of ability to self-renew. Almost 100 % of the skeleton is able to turnover per year in the first year of the human life. However this ability declines with increasing age approximately about 10 %. When the skeletal growth is completed, the bone renewal results from process called remodeling. It is a coordinated cycle of bone tissue resorption and formation. Osteoclasts, special cells, are responsible for break down and removing of old bone tissue during resorption. On the other hand, other type of cell, called osteoblasts are responsible for formation of new bone, which replacing the old one. There is no affects on the shape and density of bone during bone replacement. From the physiological point of view, it is a complex process caused by the sequence of several steps that involves osteoclasts activation, resorption of bone, osteoblasts activation and finally formation of a new bone at the site of resorption. Fractures and bone defects are also easily repaired by remodeling, but only to the size called as critical defect. In case of larger defects, medical

interventions are necessary for healing stimulation. And this is the area in which bone tissue engineering is applied [1].

2.1.2 Bone Defects Treatment Possibilities

The most likely causes of bone defects are trauma, tumor or abnormal bone development related especially with children [5]. Nowadays, there are two ways how to treat bone defects and injuries. The first and older way of treatment is use of bone grafts, highly invasive procedure. On the other hand there is a use of relatively new field called bone tissue engineering.

2.1.2.1 Bone Grafts

The technique of bone grafting was established two centuries ago. It is a surgical process involving the reparation of bone defects by bone transplantation. The transplantation could be performed by utilizing autografts or allografts. Autografts, where donor is a patient themselves, are considered to be a gold standard for bone grafts because of its histocompatibility and non-immunogenicity. In case of allografts the graft is obtain from donors [5]. There are also two another possibilities including less known isografts (from genetically identical individuals) and xenografts (from different species) [6]. Even so, autografts still have limitations such as the additional operation for obtaining the autografts, pain, morbidity and last but not least as it was said it is still invasive procedure. A few millions of people every year have to undergo this procedure every year [7].

2.1.2.2 Bone Tissue Engineering

Due to the large limits and constraints associated with bone graft transplantation, the bone engineering industry is increasingly on the rise. The goal of bone tissue engineering (BTE) is to develop new biocompatible and biodegradable materials allowing certain mechanical support that can be used to replace bone grafts in the form of rigid scaffolds or injectable paste. In addition to the development of these hi-tech materials BTE also allows their modifications, thereby achieving different chemical or physical properties [8]. As an example, modification by binding of biologically active substances, such as controlled release drugs, growth factors, or agents affecting their antimicrobial properties or mechanical properties.

In the case of BTE, composite materials are used in particular. These materials can be divided into 3 categories - non-resorbable (mostly metallic materials used mainly as joint replacements), partially resorbable materials and fully resorbable materials. Partially resorbable composites are materials consisting of a non-resorbable phase (reinforcement) and a fully resorbable matrix (e.g. Polylactic acid (PLA)/ Hydroxyapatite (HA)). Due to the use of these materials in regenerative medicine, the high demands are placed on them. These materials must be biocompatible, non-toxic, in the case of temporary implants they must be fully bioresorbable [9, 10]. Materials which exhibit excellent biodegradability have, in particular, a polymeric nature, whether biopolymers or synthetic polymers. The disadvantage is their low mechanical resistance, which is a very important parameter in BTE, especially in load-bearing bones regeneration. The highly attractive class of biomaterials are inorganic materials such as calcium phosphate ceramic, hydroxyapatite or bioglass in combination with the polymer component [10]. An example may be the injectable polymer composite pastes.

After their application, they react with the bioactive inorganic substances of the physiological fluids and give rise to tenacious bonds with natural bone, see Fig. 2. BTE is a dynamically developing branch of tissue engineering, offering many uses especially in orthopedics, traumatology and dental medicine [11].

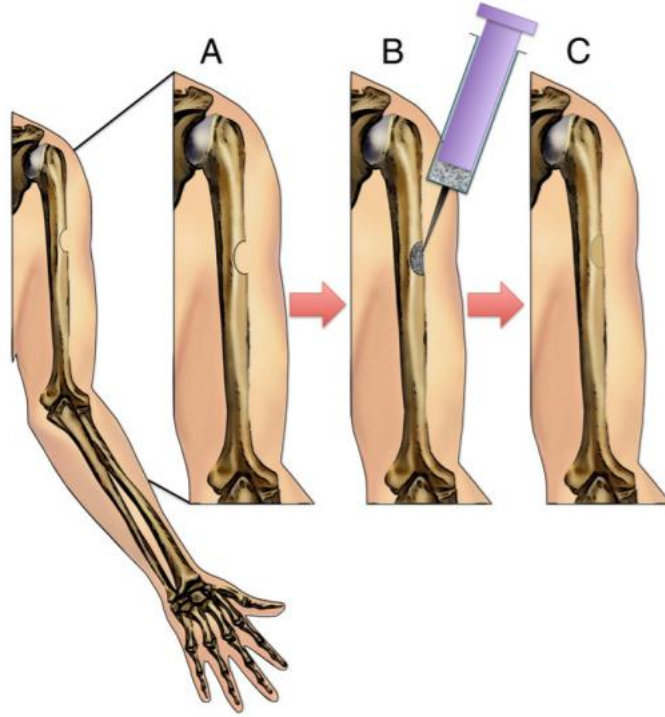


Fig. 2: Schema of bone cement application demonstrated on a humeral defect, (A) bone defect, (B) application of cement by injection, (C) remodeling and bone regeneration [8].

2.2 Calcium Phosphate Cement

Calcium phosphate cements (CPCs) are hydraulic cements producing by mixing a powder and liquid phase to form viscous and moldable paste which can be injected during surgical application using mini-invasive procedure. CPCs are also tagged as self-setting materials because of its ability to harden *in vivo* through a setting reaction at a physiological condition [12, 13, 14]. Very positive advantage is the fact that CPC setting reaction is not exothermic in comparison with acrylic bone cement used especially in arthroplasty fixation [13]. The reason is that CPC setting reaction is provided through dissolution and precipitation process. On the other hand acrylic cement harden because of exothermic polymerization reaction, which may lead to inflammatory and subsequent necrosis of the tissue according to Fernández et al. [15]. The self-setting reaction of CPC consists of three main steps: dissolution of the reactant, nucleation and growth of crystals [12].

CPCs have also several other significant and important features such great bioactivity, osteoconductivity, nontoxicity and finally they are fully resorbable [12, 16]. Discovery of calcium phosphate cements (CPCs) dates back to the 1980s. The first successful self-setting CPC was produced by Brown and Chew in the 1983 using tetracalcium phosphate (TTCP) and dicalcium phosphate dihydrate (DCPD) as a powder phase. After this CPCs started to be

widely studied. The main goal is improving and modification to achieve better properties [13].

2.2.1 Types of CPC

Three different products can be created by self-setting of CPC: Apatite, brushite and amorphous calcium phosphate (ACP). Böhner et al. found that in the case of ACP as the final product, the product was rapidly converted to calcium-deficient hydroxyapatite (CDHA). For this reason, we distinguish CPC only into two categories, namely apatite CPC and brushite CPC [12, 17].

Apatite CPCs can arise in two possible ways. In the case of monocomponent CPC it is the alpha-tricalcium phosphate (α -TCP) hydrolytic reaction to produce CDHA [18]. Another option is multi-component CPC. This is an acid-base reaction involving two or more types of orthophosphate compounds (see chapter 2.2.2). One of the reactants is always more acidic (e.g., dicalcium phosphate anhydrous (DCP), dicalcium phosphate dihydrate (DCPD)) and the second is basic (e.g., TTCP). The product of the reaction is hydroxyapatite (HA). The mechanism of both types is graphically described in Fig. 3. Unlike monocomponent CPC, the ratio of calcium and phosphorus (Ca/P) for acid-base reaction can be controlled by the ratio of acid and basic components.

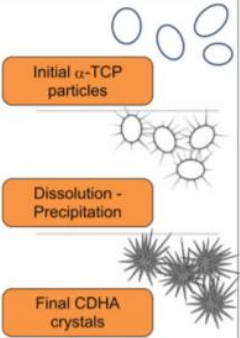
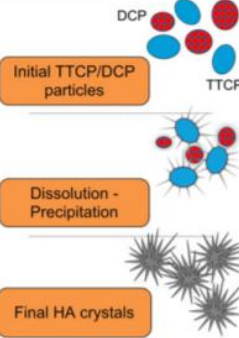
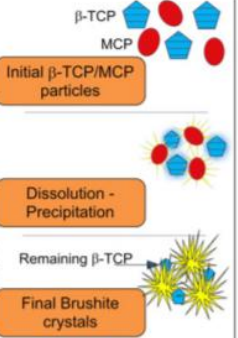
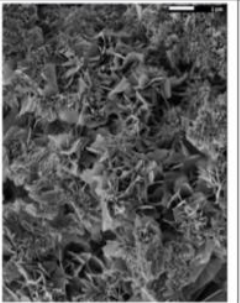
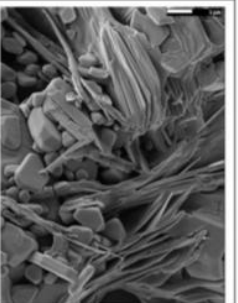
		Apatitic Cement		Brushitic Cement
		Single Component	Multiple Components	
Reactives		α -TCP	TTCP + DCPA/DCPD	β -TCP + MCPM/MCPA
Reaction		$3\alpha\text{-Ca}_3(\text{PO}_4)_2 + \text{H}_2\text{O} \rightarrow \text{Ca}_9(\text{HPO}_4)_2(\text{PO}_4)_5(\text{OH})$	$2\text{Ca}_4(\text{PO}_4)_2\text{O} + 2\text{CaHPO}_4 \rightarrow \text{Ca}_{10}(\text{PO}_4)_6(\text{OH})_2$	$\beta\text{-Ca}_3(\text{PO}_4)_2 + \text{Ca}(\text{H}_2\text{PO}_4)_2 \cdot \text{H}_2\text{O} + 7\text{H}_2\text{O} \rightarrow 4\text{CaHPO}_4 \cdot 2\text{H}_2\text{O}$
Type of Reaction		Hydrolysis	Acid-Base	Acid-Base
Setting mechanism and crystal morphology		 <p>Initial α-TCP particles</p> <p>Dissolution - Precipitation</p> <p>Final CDHA crystals</p>	 <p>Initial TTCP/DCP particles</p> <p>Dissolution - Precipitation</p> <p>Final HA crystals</p>	 <p>Initial β-TCP/MCP particles</p> <p>Dissolution - Precipitation</p> <p>Remaining β-TCP</p> <p>Final Brushite crystals</p>
			<div style="display: flex; align-items: center; justify-content: center;"> <div style="writing-mode: vertical-rl; transform: rotate(180deg);">APATITE</div> <div style="writing-mode: vertical-rl; transform: rotate(180deg);">BRUSHITE</div> </div>	
SEM				

Fig. 3: Types of CPC. Schema of possible reactions and examples of precursors using for CPCs preparation [12].

Like HA, brushite CPC is formed by an acid-base reaction. This is again a multi-component CPC. Most of the studied cements of this type were based on β -TCP (almost neutral character). As an acidic component was used monocalcium phosphate (MCP), or monocalcium phosphate monohydrate (MCPM), see Fig. 3. The final product is brushite [19]. If the reaction proceeded with excess of β -TCP, the final product would be a mixture of brushite and unreacted β -TCP. Brushite is very unstable under physiological conditions, which causes much faster resorption compared to apatite form [20].

2.2.2 Powder Phase of CPC

As the CPC powder phase, bioceramic based on calcium orthophosphates (CaP) is used. CaP compounds become very interesting in many areas of science, including chemistry, biology, medicine, etc., mainly due to its wide occurrence in nature and living organisms. The great advantage of CaP ceramics is its biocompatibility and non-toxicity to tissues [20]. In order to be used for medical purposes, it is necessary to meet other important parameters like osteoconductivity, bioactivity, crystallinity, bioresorption etc. [21]. From a chemical standpoint for CaP is composed of three basic chemical elements, calcium, phosphorus and oxygen in which last two mentioned elements form orthophosphate anion PO_4^{3-} . Based on the calcium/phosphorus (Ca/P) ratio, several compounds belonging to the calcium phosphate ceramics group are known. The overview of the individual types of CaP including their formula and the Ca/P ratio is given in Tab. 1 [20].

There are two groups of CaPs. The first group is low-temperature CaP. This type is obtained by precipitation from the solution at room temperature. Traditional use of low-temperature CaP is a precursor for the synthesis of high temperature CaP. However, with the discovery of CPC, they have also begun to be used for medical purposes because most low-temperature CaPs are found in human tissues. An example of low-temperature CaP is MCPM or dicalcium phosphate (DCP). Although MCPM is not biocompatible due to its high acidity and solubility, it is still used in medicine as part of self-hardening CPCs [22]. Even though dicalcium phosphate dihydrate (DCPD) is more bioavailable than its anhydrous form (DCP) because of its presence in pathological calcification, DCP is used to prepare CPC [20, 21].

The second group is the high-temperature CaPs, where the product is obtained at high temperature. High temperature CaPs are most commonly used for CPC preparation [17]. An example is monocalcium phosphate, tricalcium phosphate or hydroxyapatite. Monocalcium phosphate is very similar to its monocalcium phosphate monohydrate. Although it is an anhydrous form and like MCPM is not biocompatible, it can be used as part of CPC in combination with basic CaP. Its wider use prevents hygroscopicity. TCP is polymorphic, which means it occurs in three crystallographic modifications, α -TCP, α' -TCP (due to poor property unusable and uninteresting) and β -TCP. There are several ways to synthesize β -TCP. One is, for example, thermal decomposition of CDHA at a temperature higher than 800 °C. At a temperature above 1125 °C, however, it changes to α -TCP. In room temperature, β -TCP phase is less soluble than α -TCP. In calcified tissues, pure β -TCP is not present, only its magnesium substituted form. Even though it is not found in biological tissues itself, it is used in medicine. For the preparation of CPC, α -TCP is also used, although it has the disadvantage of a very fast desorption over β -TCP, more precisely desorption occurs faster than new tissue

formation. Another very interesting and most commonly used type of CaP is hydroxyapatite. It is the most crystalline, most biocompatible and most stable CaP compound in the aqueous solution. Chemically it is very similar to the mineral contained in bones and teeth. For this reason, it is commercially widely used in medicine not only as a part of CPC [20].

Tab. 1: CaP compounds and their major properties [13, 17, 20].

Name	Abbreviation	Formula	Ca/P ratio	Solubility at 25 °C, log(Ks)
Monocalcium phosphate monohydrate	MCPM	$\text{Ca}(\text{H}_2\text{PO}_4)_2 \cdot \text{H}_2\text{O}$	0.5	1.14
Monocalcium phosphate	MCP	$\text{Ca}(\text{H}_2\text{PO}_4)_2$	0.5	1.14
Dicalcium phosphate	DCP	CaHPO_4	1.0	6.90
Dicalcium phosphate dihydrate	DCPD	$\text{CaHPO}_4 \cdot \text{H}_2\text{O}$	1.0	6.59
Octacalcium phosphate	OCP	$\text{Ca}_8\text{H}_2(\text{PO}_4)_6 \cdot 5\text{H}_2\text{O}$	1.33	96.6
α -Tricalcium phosphate	α -TCP	$\text{Ca}_3(\text{PO}_4)_2$	1.5	25.5
β -Tricalcium phosphate	β -TCP	$\text{Ca}_3(\text{PO}_4)_2$	1.5	28.9
Calcium-deficient hydroxyapatite	CDHA	$\text{Ca}_9(\text{HPO}_4)(\text{PO}_4)_5(\text{OH})$	1.5-1.67	~85
Hydroxyapatite	HA	$\text{Ca}_{10}(\text{PO}_4)_6(\text{OH})_2$	1.67	116.8
Tetracalcium phosphate	TTCP	$\text{Ca}_4(\text{PO}_4)_2\text{O}$	2.0	38-44

An important feature for CPC preparation is also solubility that provides relatively valuable information about the potential behavior of CaP in an aqueous in vivo environment. Depending on the rate of dissolution, the orthophosphate compounds may be ordered:

$$\text{MCPM} > \text{TTCP} \approx \alpha\text{-TCP} > \text{DCPD} > \text{DCP} > \text{OCP} > \text{TCP} > \text{CDHA} > \text{HA}. [13]$$

2.2.3 Liquid Phase of CPC

Pure water, physiological saline [18, 23, 24], or aqueous solutions of synthetic polymers and biopolymers can be used as the liquid phase [25]. Adier et al used sodium hydroxide solution as an aqueous phase [26]. Polycarboxylic acid (PCA) was used by Myiazaki et al. [27]. The reason why polymer solutions have been increasingly used in recent years is to improve the injectability of the pastes. Hesaraki et al. as the liquid phase, hyaluronic acid and polyethylene glycol. In both cases, CPC showed improved injectability compared to the use of distilled water which caused the phase separation of the paste [28]. Biodegradable and thermosensitive polymers have great potential in this field [8, 29].

2.2.3.1 Temperature Responsive Triblock Copolymer

Thermally sensitive polymers have become very interesting as injectable drug carriers. These polymers have the ability to react to small temperature changes by the formation of physically cross-linked hydrogels. This is a reversible sol-gel transition. We include, for example, Poloxamer or PLGA-PEG-PLGA triblock copolymer as a triblock thermoplastic copolymer. [32]. Both were studied in connection with the CPC. Poloxamer is poly(ethylene glycol-*b*-propylene glycol-*b*-ethylene glycol) [29, 30, 31]. Unlike the PLGA-PEG-PLGA copolymer, Poloxamer is not biodegradable. Higher concentrations show toxicity [32].

Among the biodegradable triblock copolymers are the above mentioned aliphatic PLGA-PEG-PLGA copolymer, commercially known as ReGel[®]. It is a copolymer based on hydrophilic poly (ethylene glycol), as a central molecule and poly (lactic-*co*-glycolic acid). Its formula is shown in Fig. 4. It shows excellent biocompatibility and biodegradability. Under physiological conditions, they undergo hydrolysis to produce metabolites (lactic acid and glycolic acid) which are further subject to degradation in the Krebs cycle to water and carbon dioxide. A very interesting feature is their thermosensitivity. It is an ability of reversible sol-gel transition in aqueous solution under physiological conditions (see Fig. 5). The PLGA-PEG-PLGA copolymer has an amphiphilic character (hydrophobic and hydrophilic component) which is susceptible to the formation of micelles in an aqueous medium. Due to its properties, the PLGA-PEG-PLGA aqueous solution has a great potential just as part of the injectable CPC [32-35]. Another advantage of the PLGA-PEG-PLGA copolymer is the possibility of its modification (e.g., itaconic acid), which can be used, for example, to bind bioactive substances (e.g., drugs, growth hormones) [34].

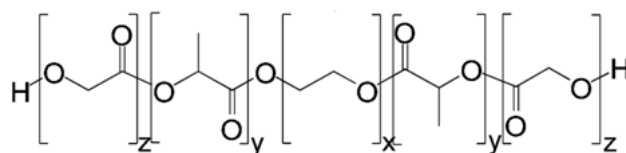


Fig. 4: Schema of PLGA-PEG-PLGA triblock copolymer.

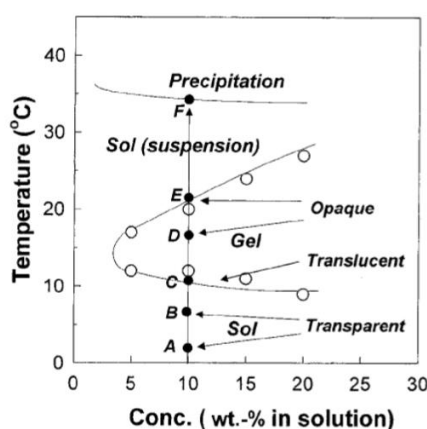


Fig. 5: Phase diagram of aqueous solution of PLGA-PEO-PLGA triblock copolymer.

2.2.4 Additives for CPC

The advantage of CPC traps is the ability to customize their properties with a potential application. It is possible to adjust the chemical, physical and biological properties. Physical properties (time and rate of setting, cohesion, injectability, etc.) can be adjusted to a certain extent by, for example, varying composition, L/P ratio, particle size etc. (see chapter 2.4). Another option is to use additives. Because of the use of CPC for biomedical purposes, any compound exhibiting biodegradability, biocompatibility and non-toxicity can be considered as an additive. They can be part of both powder and liquid phases. Additives can be biologically active substances (e.g., drugs, growth factors, and also the polymer component added by the liquid phase (see chapter 2.2.3). The most frequent reason for finding new additive options, however, remains one of the mentioned physical and mechanical properties. The list of studied additives is given in Tab. 2.

Tab. 2: Possible additives and their effects on CPC properties.

Additive	Paste composition	Effects	Ref.
Hyaluronic acid (HAc)	β -TCP+water	Increase viscosity and thixotropy, improving injectability.	[28]
	α -TCP+aq. $\text{NaH}_2\text{PO}_4 \cdot 2\text{H}_2\text{O}$	No interesting features	[25]
Hyaluronan-bisphosphate (HABS)	α -TCP+aq. $\text{NaH}_2\text{PO}_4 \cdot 2\text{H}_2\text{O}$	Improving cohesion Increasing cement toughness	[25]
Sodium Carboxymethyl Cellulose (CMC)	α -TCP+aq. $\text{NaH}_2\text{PO}_4 \cdot 2\text{H}_2\text{O}$	Improving cohesion	[25]
Polyethylenglycol (PEG)	β -TCP+water	Increase viscosity Improving injectability.	[28]
	ACP+DCPD+water	Reduction injectability, setting time.	[36]
Disodium hydrogen phosphate (DHP)	ACP+DCPD+water	Augmentation of injectability and setting time.	[36]
Glycerin	ACP+DCPD+water	Reduction of injectability and setting time.	[36]

Additive	Paste composition	Effects	Ref.
Citric acid (CA)	ACP+DCPD+water	Reduction of injectability and setting time. Causing inflammation	[36]
Chitosan ^b (0.4 wt %)	ACP+DCPD+water	Reduction of viscosity Augmentation of anti-wash out property	[37]
Chitosan	Cementek ^c	Slightly improving injectability and strength Increasing setting time	[38]
Glycerol	Cementek	Improving injectability Increase setting time Decrease mechanical property	[38]
Lactic acid	Cementek	Improving injectability Setting time reduction Increasing toughness Dissolution rate limitation	[38]
Sodium glycerophosphate	Cementek	Improving injectability Necessary for CPC homogeneity	[37]
Sodium alginate ^b (0.4 wt %)	ACP+DCPD+water	Increasing compressive strength and anti-wash out property	[37]
Modified starch ^b (0.4 wt %)	ACP+DCPD+water	Increasing compressive strength, excellent anti-wash out property	[37]

a) only 0.75 wt % HABS, b) only for conc. 0.4 wt %, c) commercial mark (see chapter 2.2.6)

For the purpose of our research, dopamine was used as an additive. Due to its very attractive features, it seems to be a suitable candidate for improving not only rheological and mechanical proprietary CPCs.

2.2.4.1 Dopamine

Attention to dopamine (DOPA) has been attracted by the mussels, aquatic organisms able to adhere strongly to any surface in the water. This remarkable ability to adhere to the surface has become the inspiration for material engineering. Mussels produce thin fibers containing an adhesive. Where the plaque comes into contact with the surface, there are proteins called "mussel foot" proteins (Mefp). These proteins are largely made up of lysine and 3,4-

dihydroxy-L-phenylalanine. For this reason, it was concluded that the adhesions were mainly responsible for catechol DOPA [39, 40].



Fig. 6: Mussel attached to the surface of a piece of brick by plaque fibers [41].

Dopamine is a chemical belonging to catecholamines. It is a simple organic molecule containing catechol and amine group. Under certain conditions, dopamine is capable of polymerizing, which makes it possible to form a layer on the surface of the most diverse materials. By covalent and non-covalent bonds strongly adherent to a given material [40].

Several mechanisms of dopamine polymerization are known [39]. Dopamine is capable of polymerizing spontaneously self-polymerization in the presence of oxygen (oxidizing agent) and at $\text{pH} > 7.5$. Polymerization of dopamine occurs in solution and is a mild reaction requiring no complicated apparatus and harsh conditions. Once the DOPA monomers are added to the alkaline solution, the polymerization process is started immediately. Briefly, the entire polymerization process begins by oxidation of DOPA to 5,6-dihydroxyindole (DHI) over several intermediates. Then there are two competing reactions. The first reaction is covalent polymerization and formation of oligomers. The second reaction is of a non-covalent nature. This involves the binding of the unreacted monomer to the oxidized form of DHI and subsequent formation of the trimer. The products of these reactions produce non-covalent interaction and result in the resulting polydopamine. The DOPA polymerization scheme is described in Fig. 7 [40].

As described above, dopamine polymerizes in the presence of oxygen as oxidizing agent. A disadvantage of polymerization under these conditions may be the lack of oxygen diffusion deeper into the volume of the substrate. One possible solution is to use dissolved sodium iodate as oxidizing agent [42].

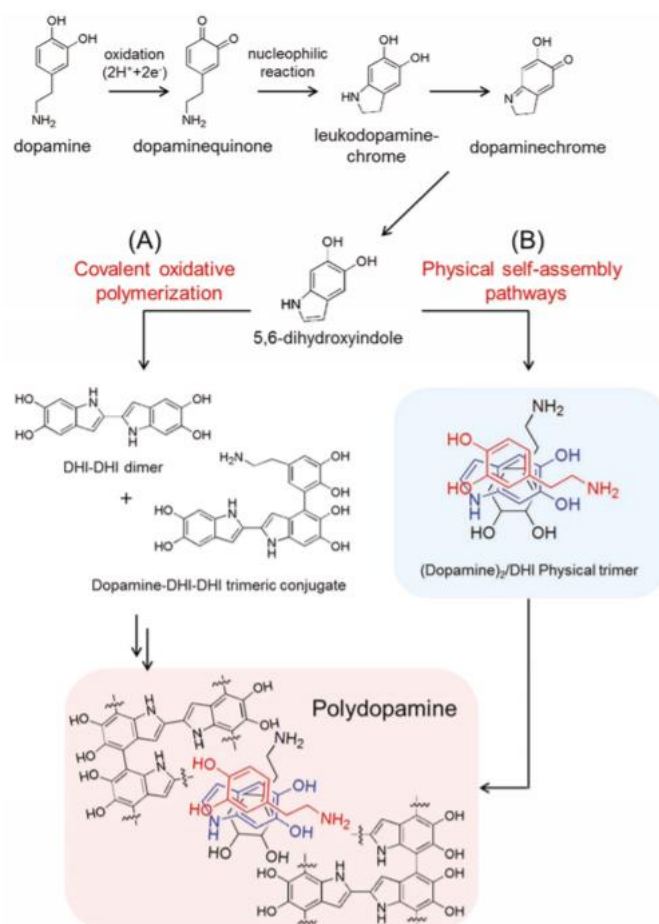


Fig. 7: The schema of DOPA polymerization reaction [40].

From a biological point of view, dopamine is known as a neurotransmitter and a hormone. This is a fully biocompatible substance. The same property was confirmed in polydopamine. Study Ku et al. showed that polydopamine did not endanger the viability of cells such as fibroblasts, neurons, or osteoblasts. On the contrary, it has been found that, on application of polydopamine coatings, it promotes adhesion of cells [40]. It also shows negligible cytotoxic properties [43]. For the time being, polydopamine has been investigated in connection with biomedical applications as a coating of materials and scaffolds, e.g., for nerve [44], bone [45, 39], or skin cells [46].

2.2.4.2 Selenium Nanoparticles

In the 1950s selenium was found to be essential element for living organisms. This means that it is necessary to receive it in the diet or as a food supplement. Selenium has been found to exhibit many positive effects for the human organism. In the body, for example, it acts as an antioxidant and protects cells and tissues from damage. With the advent of nanotechnology, the synthesis of selenium nanoparticles has become very attractive not only with nutraceuticals but also with medical applications. The advantage of selenium nanoparticles is their chemical stability, biocompatibility and low cytotoxicity. The ability to modify selenium by biopolymers (e.g., chitosan) can be considered very positive. It can be used for gradual

release of selenium, or for use as antibacterial or anticancer agents. For these reasons, selenium nanoparticles have great potential in the treatment of diseases [47].

2.2.5 Biomedical Application of CPC

Because of their excellent formability and other features, CPC is the subject of many studies of their application in medicine as temporary replacement of bone tissue. Their potential increases the fact that they can be injected with a mini-invasive procedure. A great benefit is particularly in orthopedics and traumatology, where they are studied as a possible method of fixation of fractures, or in arthroplasty as adhesives for hip joint replacement [25]. O'Hara et al. studied the use of CPC for spinal bone repair in vertebroplasty and kyphoplasty [13]. In contrast, Kodera et al. deal with use of CPC use in neurosurgery for cryoplasty [48]. They can be widely used in reconstructive surgery, dentistry, or as drug carriers [49]. An interesting study was carried out by Heseraki et al., who are involved in the application of CPC in the treatment of soft tissues. Specifically their studies concerned on vesicoureteral reflux treatment [28].

2.2.6 Commercially Available CPC

Bohner et al. created a list of commercially available CPC pastes including their composition. It is clear from Tab. 3 that apatite type cement is used for medical purposes. The primary precursor is most often α -TCP in combination with types not only of CaP bioceramics. A relatively few CPC are available in the market [20]. CPC is still a subject of long-term study. The aim is to continually improve the quality and achieve the best chemical, physical and biological properties that are subject to stringent requirements and need to adapt them to future applications [50].

Tab. 3: Commercial calcium phosphate cements with their composition (when available) [50].

Company	Cement name	Components	End-product
ETEX	α -BSM	<i>Powder:</i> ACP (50 %), DCPD (50 %) <i>Solution:</i> H ₂ O (unbuffered saline solution)	Apatite
	Embarc		
	Biobon		
Stryker-Leibinger Corp.	BoneSource	<i>Powder:</i> TetCP (73 %), DCP (27 %) <i>Solution:</i> H ₂ O, mixture of Na ₂ HPO ₄ and NaH ₂ PO ₄	Apatite
Teknimed	Cementek®	<i>Powder:</i> α -TCP, TetCP, Na Glycerophosphate <i>Solution:</i> H ₂ O, Ca(OH) ₂ , H ₃ PO ₄	Apatite
	Cementek® LV	<i>Powder:</i> α -TCP, TetCP, Na Glycerophosphate, dimethylsiloxane <i>Solution:</i> H ₂ O, Ca(OH) ₂ , H ₃ PO ₄	Apatite

Company	Cement name	Components	End-product
Biomet	Calcibon® (previously called „Biocement D“)	<i>Powder:</i> α -TCP (61 %), DCP (26 %) CaCO_3 (10 %), PHA (3 %) <i>Solution:</i> H_2O , Na_2HPO_4	Apatite
	Mimix™	<i>Powder:</i> TetCP, α -TCP, $\text{C}_6\text{H}_5\text{O}_7\text{Na}_3 \cdot 2\text{H}_2\text{O}$ <i>Solution:</i> H_2O , $\text{C}_6\text{H}_8\text{O}_7$	Apatite
	QuickSet Mimix™	<i>Powder:</i> nf ^a <i>Solution:</i> nf ^a	Apatite
Mitsubishi materials	Biopex®	<i>Powder:</i> α -TCP (75 %), TetCP (20-18 %), DCPD (5 %), HA (0–2 %) <i>Solution:</i> H_2O , sodium succinate (12-13 %), sodium chondroitin sulphate (5-5.4 %)	Apatite
	Biopex®-R	<i>Powder:</i> α -TCP, TTCP, DCPD, HA, $\text{Mg}_3(\text{PO}_4)_2$, NaHSO_3 <i>Solution:</i> H_2O , sodium succinate, sodium chondroitin sulphate	Apatite
Kyphon	KyphOs™	<i>Powder:</i> α -TCP (77 %), $\text{Mg}_3(\text{PO}_4)_2$ (14 %), MgHPO_4 (4.8 %), SrCO_3 (3.6 %) <i>Solution:</i> H_2O , $(\text{NH}_4)_2\text{HPO}_4$ (3.5 mol dm^{-3})	Apatite
Skeletal Kinetics	Callos™	<i>Powder:</i> nf ^a <i>Solution:</i> nf ^a	Apatite
Shanghai Rebone Biomaterials Co, Ltd ^b	Rebone	<i>Powder:</i> TetCP, DCP <i>Solution:</i> H_2O	Apatite
Synthes-Norian	Norian® SRS Norian® CRS	<i>Powder:</i> α -TCP (85 %), CaCO_3 (12 %) MCPM (3 %) <i>Solution:</i> H_2O , Na_2HPO_4	Apatite
	Norian® SRS Fast Set Putty Norian® CRS Fast Set Putty	<i>Powder:</i> nf ^a <i>Solution:</i> nf ^a	Apatite
	chronOS™ Inject	<i>Powder:</i> β -TCP (73 %), MCPM (21 %), $\text{MgHPO}_4 \cdot 3\text{H}_2\text{O}$ (5 %), MgSO_4 (< 1 %), $\text{Na}_2\text{H}_2\text{P}_2\text{O}_7$ (< 1 %) <i>Solution:</i> H_2O , sodium hyaluronate (0.5 %)	Brushite
Kasios	Eurobone®	<i>Powder:</i> β -TCP (98 %), $\text{Na}_4\text{P}_2\text{O}_7$ (2 %) <i>Solution:</i> H_2O , H_3PO_4 (3.0 mol dm^{-3}), H_2SO_4 (0.1 mol dm^{-3}) [58]	Brushite

Company	Cement name	Components	End-product
CalciphOs	VitalOs ^c	<i>Component 1:</i> β -TCP (1.34 g), $\text{Na}_2\text{H}_2\text{P}_2\text{O}_7$ (0.025 g), H_2O , salts ($0.05 \text{ mol}\cdot\text{dm}^{-3}$, pH 7.4 PBS slution) <i>Component 2:</i> MCPM (0.78 g), $\text{CaSO}_4 \cdot 2\text{H}_2\text{O}$ (0.39 g), H_2O , H_3PO_4 ($0.05 \text{ mol}\cdot\text{dm}^{-3}$)	Brushite

The end-product of the reaction can be either an apatite (calcium-deficient, carbonated, etc.) or brushite.

a) Not found in the literature or on the web.

b) Assumed composition based on the scientific literature.

c) The cement consists of two liquids in which the various powder components are dispersed.

2.3 Rheology

The word rheology was first introduced in 1920 by Professor Bingham. Rheology is a field of science dealing with flow and deformation of matter. Its subject is the characterization of flow properties, which are an important parameter in the processing of material. The measurement of rheological properties can be applied to all types of systems such as liquids (polymer solution), semi-solids (polymer melts) and solids (composites). Their properties are related to their molecular structure and conditions such as temperature. Rheology is a widely used and important method of characterization in various industries (e.g., plastics, pharmaceutical, cosmetics, and food industries) [51].

Two extreme types of ideal material behavior are known depending on external mechanical forces - elastic behavior and viscous behavior. Elastic behavior is characterized by the fact that after removal of mechanical forces the deformation disappears and the object returns to its original state. On the other hand, when applying mechanical forces for the viscous behavior, a flow occurs. This flow stops after the forces are removed. There is no reversible reaction at which the body would be returned to its original state.

In the case of polymers, whether we are talking about melts, dispersions or polymer solutions, the response to applied stress is partially elastic and partially viscous. In this case, it is a so-called viscoelastic behavior, which is a function of time and temperature.

Based on flow behavior, materials can be divided into two systems - Newtonian and Non-Newtonian fluids [52].

2.3.1 Newtonian Fluid

Newtonian fluids are those whose viscosity is dependent only on temperature, not on shear stress and time. Such behavior is governed by Newton's law, which considers the linear dependence between the applied shear stress τ (Pa) and the shear rate $\dot{\gamma}$ (s^{-1}) [52]. The most frequent case of this type is the increase in viscosity with pressure and conversely its decrease with temperature. Liquids that exhibit Newtonian behavior include, in particular, low-molecular substances (e.g., water). In the case of polymeric systems, such behavior exhibits polymer solutions otherwise known as sol phase [51].

2.3.2 Non-Newtonian Fluid

In the case of Non-Newtonian fluids the viscosity is not constant but is a function of shear rate or shear stress respectively. In other words, the ratio of shear stress and shear rate is not a material constant, since it varies with the shear stress. This ratio is called apparent viscosity. This viscosity is not sufficient to characterize the flow properties and therefore the flow properties are assessed by compiling flow curves that describe the viscosity of the material at a wider shear rate interval. Due to the fact that the viscosity also varies with temperature, it is necessary that the measurements take place at a constant temperature and the sample has been properly tempered. In the case of comparison of the materials with one another, it is therefore desirable that the individual measurements take place at the same temperature. If this condition is not met, the flow curves are incomparable. Beside that the apparent viscosity is a function of flow parameter, it also depends on the kinematic history of the material [52].

Non-Newtonian systems are described by a power relationship, also known as the Ostwald-de Waele relationship:

$$\tau = K \cdot \dot{\gamma}^n, \quad (1)$$

where K is the flow consistency index and n is the flow behavior index. The flow behavior index represents the degree of diversion of the flow curve from the Newtonian course. Based on the value of n , non-Newtonian fluids can be divided into pseudoplastic ($n < 1$) and dilatant ($n > 1$). Special types are so-called Bingham fluids. For these fluids, the shear deformation starts only after a certain shear stress has been exceeded. These substances can behave both as Newtonian (Bingham plastic fluid) and non-Newtonian (viscoplastic behavior). The flow curves of each type of behavior are shown in Fig. 8. All these types of behavior are referred as time independent, which means they do not have a shape memory [51].

Time-dependent fluids are more complicated cases where the apparent viscosity is time-dependent. Two cases of such behavior are known - thixotropic and reopex behavior. Thixotropy is characterized by a decrease in the apparent viscosity with the shear stress duration [53]. When the shear stress stops the apparent viscosity increases. Reopexia is the opposite example when the apparent viscosity increases with shear stress. In both cases, flow curves have the character of a hysterical loop. The temporal dependence of the apparent viscosity can also be caused by chemical reactions. In connection with this work we can mention the cement self-setting as an example of thixotropic behavior [52].

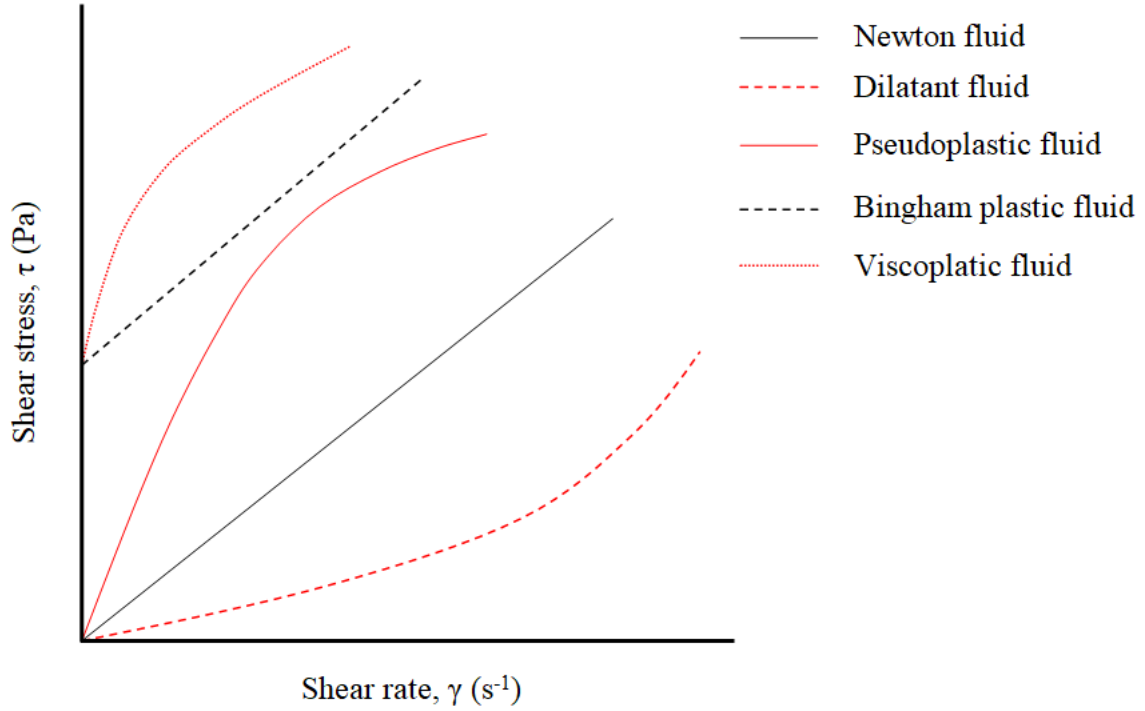


Fig. 8: Flow curves of time independent types of fluids. Reformed by [16].

2.4 Rheology of CPC

Rheological behavior is one of the most important topics in the context of research and development of bone adhesives based on CPC. Proper understanding and study of these properties is very important for several reasons [54]. Using rheology, it is possible to characterize process and application parameters such as injectability, cohesion, application time, self-hardening time and its CPC course [50, 54]. Injectability is the ability of the material to be extruded through a thin and long needle. Therefore, the paste must be sufficiently viscous but at the same time stable and compact to avoid phase separation [17]. O'Neill et al. in their study are focused precisely on the problems of rheological properties and in particular injectability [16, 54]. Cohesion is characterized as the ability to harden in the aquatic environment without disintegration into small particles [7].

The reason for an important understanding of the basic features of CPC is the fact that CPC is a time dependent reactive system which undergoes continuous transformation from fluid to solid state. During this transformation, its viscoelastic properties also change, which is depending on evaluation of internal microstructure based on three-dimensional network. Networks and microstructures are formed that affect not only flowability (injectability), but also mechanical properties of cements after setting. The resulting mechanical properties are dependent also on other parameters such as final paste composition or liquid-powder (L/P) ratio. Graphical representation of the CPC self-setting progress is shown in Fig. 9. It is obvious, therefore, that the self-hardening process has several periods. From application point of view, it is very important to know the duration of these periods. This is also fundamental reason for studying CPCs rheological properties. The duration of the period may be

influenced by acceleration/deceleration by adjusting the rheological properties of the CPC. This can be achieved by adding suitable additives (see chapter 2.2.4), by adjusting the L/P ratio or by the roughness, shape, size and time of milling of the powder phase. It follows from the above that self-setting of CPC is due to chemical reactions. This results to thixotropic behavior of CPC [54].

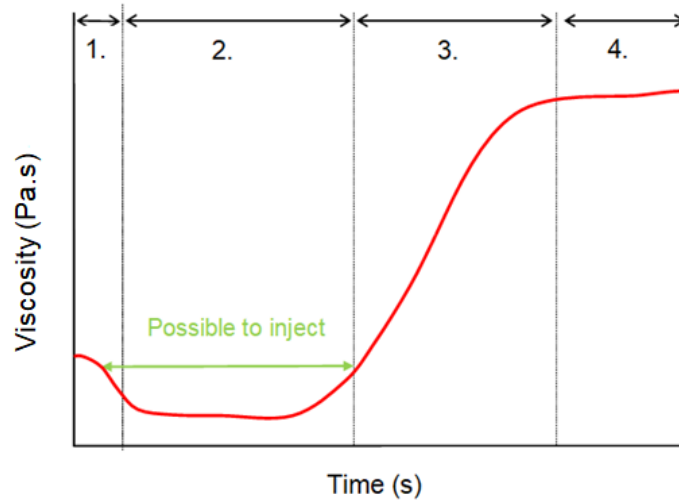


Fig. 9: The course of setting of CPC. 1. processing period, 2. working period, 3. setting period, 4. final hardening period.

2.4.1 Viscoelastic Behaviour Measurement of CPC

For measurement of rheological properties and viscoelastic behavior of CPC, rheological measurement is used. For kinetics of the curing reaction and the associated time-dependent changes in viscoelastic properties, it is appropriate to use a rotary rheometer (see Fig. 10) and submit a sample to dynamic analysis and steady state analysis [39].



Fig. 10: Rotational rheometer (TA Instruments) [56].

To characterize the viscoelastic properties of a rotary rheometer, it is important to choose a suitable geometry. The most common types of geometry are concentric cylindrical, cone plate and parallel plate. Concentric cylindrical geometry is most commonly used for very viscous liquids. For our system, the most appropriate variant is cone plate or parallel plate geometry (see Fig. 11). Cone plate geometry is suitable for low to medium viscosity fluids. Its advantage is that shear rate and stress are constant across the whole geometry gap. If this geometry is used to analyze material containing particles, it is necessary that the particle size reaches a maximum 1/10 of the distance between the cone and plate. Parallel plate geometry is suitable for low and medium viscosity fluids, soft solids and also filled materials containing larger particles than can be used with the cone plate geometry. The disadvantage of this type of geometry is the uneven distribution of shear stress and rate. The trend is such that the maximum shear values are at the edges of the geometry, while the minimum shear value is along the vertical axis of the geometry [57].

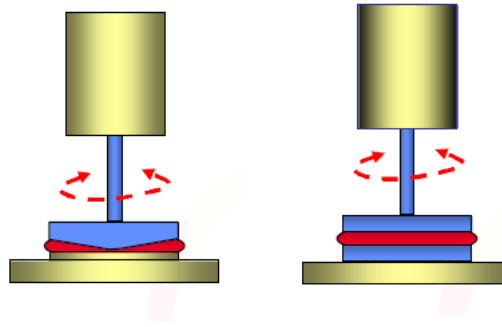


Fig. 11: Types of geometry used for dynamic rheological analysis. Cone plate geometry and parallel plate geometry (from the left side) [58].

2.4.1.1 Dynamic Oscillatory Testing

For the measurement of linear viscoelastic region (LVR) the oscillation testing method is used. Small amplitude sinusoidal oscillation is applied to the sample during dynamic oscillation. After that the resulting stress (τ) is compared with strain (γ) [39]. The strain wave of viscoelastic material is shifted by δ between $\frac{\pi}{2}$ and 0. This phenomenon can be mathematically described:

$$\begin{aligned}\gamma &= \gamma_0 \sin(\omega t), \\ \tau &= \tau_0 \sin(\omega t + \delta)\end{aligned}\tag{2}$$

Where γ_0 is amplitude of strain, τ_0 is amplitude of stress, ω is angular frequency and t is time. It is possible that the shifted stress wave can be broken into two waves. The first one is in phase with strain (τ') and the second one is shifted by $\frac{\pi}{2}$ (τ''). Then, one can write:

$$\tau = \tau' + \tau'' = \tau_0' \sin(\omega t) + \tau_0'' \cos(\omega t) \quad (3)$$

It follows that $\tan \delta$ can be defined as:

$$\tan \delta = \frac{\tau_0''}{\tau_0'} \quad (4)$$

Phase difference δ indicating the storage G' and loss G'' modulus (see equation (6)). G' is a characterization of elastic behavior and G'' represents viscous behavior of viscoelastic material. Mathematically, these modules can be derived from the Hook's law:

$$\begin{aligned} G' &= \frac{\tau_0'}{\gamma_0} \\ G'' &= \frac{\tau_0''}{\gamma_0} \end{aligned} \quad (5)$$

By combination of equation (4) and (5), one can obtain [59]:

$$\tan \delta = \frac{G''}{G'} \quad (6)$$

During the oscillatory testing, it is very important to perform the experiment in the linear viscoelastic region, where G' and G'' is not dependent on maximum amplitude of strain, stress or frequency [60]. If the experiment is performed in the linear region G^* is constant. If the experiment is set outsider the linear region G^* is a function of the shear rate and angular frequency. In connection with oscillatory testing, strain sweep, frequency sweep, temperature sweep, or time sweep are used. Their overview and measurement conditions are listed in Tab. 4. Time sweep is very useful for CPC characterization, as it maps the progress of self-setting of pastes [54].

To ensure that the experiment runs in linear region, it is necessary to determine the strain or frequency range in which the linear region is located. Therefore, it is always necessary to first measure Strain sweep for the material to be studied. After that, it is needed to choose some value belonging to the linear viscoelasticity region (see Fig. 12) and then use it as a parameter for frequency sweep measurement. From the frequency sweep output, the frequency value also belonging to the linear region is selected. Experimentally detected strain and frequency parameters are used for subsequent characterization of CPC samples. The change in rheological properties is no longer conditioned by conditions, but is actually based on the development of the CPC structure [19, 23].

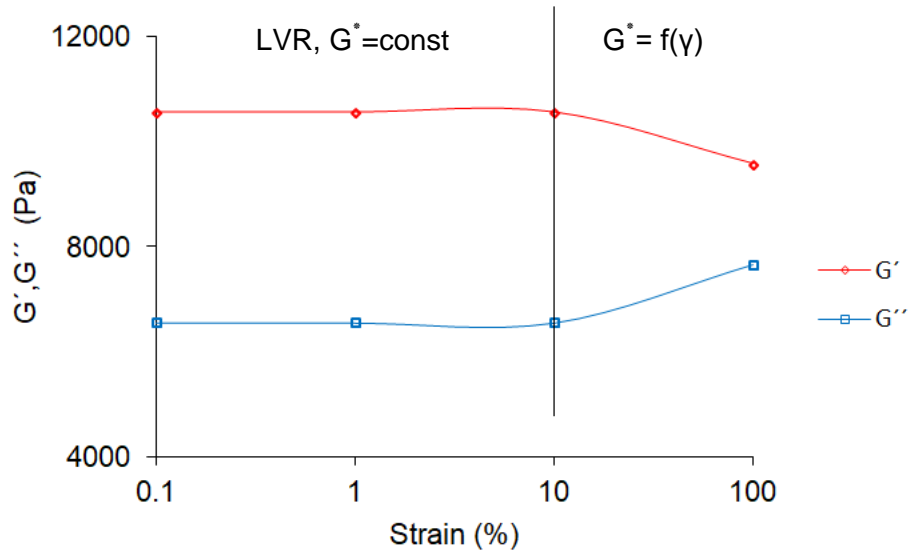


Fig. 12: Characterization of linear viscoelastic region (LVR), where modulus is independent of strain.

Tab. 4: Type of dynamic rheological testing methods [55].

Type of testing	Constant parameters	Changing parameters
Strain sweep	Frequency, temperature	Strain
Frequency sweep	Strain, temperature	Frequency
Time sweep	Strain, frequency, temperature	Time
Temperature sweep	Strain, frequency	Temperature

2.4.1.2 Steady State Testing

The principle of steady rheology is the measurement of the shear stress during a linear increasing (decreasing) shear rate. A thixotropic behavior is characteristic of this testing. As already outlined in chapter 2.3.2, thixotropy is manifested by a decrease in apparent viscosity with increasing shear velocity. The output of thixotropic behavior measurement is a hysteresis loop [23].

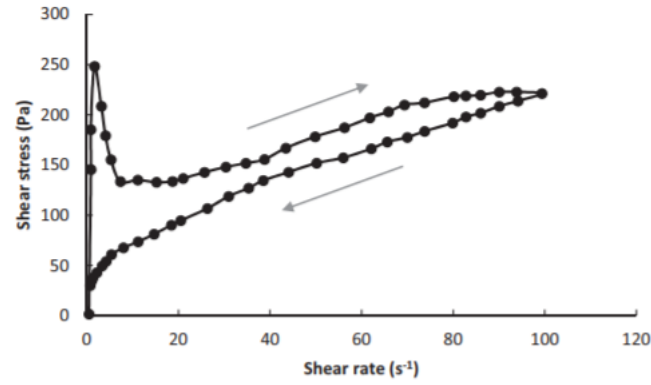


Fig. 13: Shear stress and shear rate relation of CPC [53].

Green and Weltaman were the first to introduce a technique of hysterical loop. The technique consisted in systematically increasing and decreasing the shear rate from zero to the maximum achievable value. The area between the curves is a characteristic of thixotropy. Both the area and the shape of the loop vary depending on the materials and it is also connected with condition such as shear history [53].

3 MAIN GOALS OF THE WORK

The main goal of the diploma thesis is to study changes of viscoelastic properties of the polymer-composite bone pastes based on the PLGA-PEG-PLGA thermosensitive triblock copolymer solution and calcium phosphate bioceramics as a powder phase, in comparison with those that are modified by selected additives and explaining whether and how additives influence the setting reaction. The individual steps of proposed master's thesis can be summarized as follows:

1. Optimization of setting and parameters for rheological analyses of calcium phosphate pastes.
2. Dynamic rheological behavior (temperature sweep) and steady state properties of PLGA-PEG-PLGA triblock copolymer.
3. Dynamic rheological behavior (frequency, strain and time sweeps) and steady state properties of unmodified calcium phosphate pastes and also pastes modified with dopamine, sodium iodate and selenium nanoparticles.
4. Comparing and discussing effects additives on thixotropic behavior and kinetics of setting reaction.

4 EXPERIMENTAL PART

4.1 Chemicals

- PLGA-PEG-PLGA triblock copolymer (was prepared by Bc. Simona Debnárová at CEITEC, BUT Brno).
- Ultrapure water (Ultrapure water of Type I according to ISO 3696) was prepared on Millipore purification system (MilliQ Academic, Millipore, France).
- Calcium Phosphate monobasic ($\text{H}_4\text{CaO}_6\text{P}_2$, $\geq 95\%$) was purchased from Sigma-Aldrich, Germany
- Alpha-Tricalcium Phosphate ($\text{Ca}_3(\text{PO}_4)_2$, $>95\%$) was purchased from Premier Biomaterials, Ireland
- Dopamine hydrochloride was purchased from Sigma-Aldrich, Germany
- Sodium Iodate (NaIO_3 , $\geq 98\%$) was purchased from Penta s.r.o., Czech Republic
- Tris(hydroxymethyl)aminoethane ($\geq 99.8\%$) was purchased from Sigma-Aldrich, Germany
- Solution of selenium nanoparticles (SeNPs), prepared by MENDELU, Brno.
- Silicon oil DC 704, density at 25 °C is $1070 \text{ kg}\cdot\text{m}^{-3}$, origine unknown.
- Liquid nitrogen was purchased from Linde Gas, a.s., Czech Republic.

4.2 Equipments

- Rheometer AR-G2 (TA instruments)
- Micropipette (Laborgeräte Hirschmann)
- Water proof pocket-size pH Meter S2K712 with ISFET sensors (ISFET Company, Japan)
- Analytical scale AB204-S (Mettler-Toledo, s.r.o, Czech Republic).
- Vacuum drying oven (Vacucell 22, BMT a.s., Czech Republic)
- Proton Nuclear Magnetic Resonance - 700 MHz NMR spectrometer Bruker AVANCE III at Masaryk University (Bruker Co., Germany)
- Laser Particle Sizer Analyzer LA-950 (Horiba, Japan)
- Scanning Electron Microscope MIRA3/XMU (Tescan, Czech Republic)
- Sputter coater Leica EM ACE600 (Leica, Germany)
- Elix® Essential 5 (Merck Millipore Co., Germany)
- Dynamic light scattering DynaPro NanoStar (Wyatt Technology, USA)

4.3 Methods

4.3.1 Synthesis and Purification of PLGA-PEG-PLGA Copolymer

Thermosensitive poly(D,L-lactic acid-*co*-glycolic acid)-*b*-poly(ethylene glycol)-*b*-poly(D,L-lactic acid-*co*-glycolic acid) triblock copolymer (PLGA-PEG-PLGA) with LA/GA molar ratio equal to 3.0 and PLGA/PEG weight ratio equal to 2.5 was synthesized under nitrogen atmosphere via ring opening polymerization method in a bulk at 130 °C according to Michlovská et al. [34].

4.3.2 Preparation of PLGA-PEG-PLGA Copolymer Solution

PLGA-PEG-PLGA aqueous solution with concentration equals to 20 w/v % (in the next text it will be donated as 20% solution) was prepared by dissolving in ultrapure water for approximately 48 hours. The sample was stirred in cold bath in the temperature range from 13 to 18 °C. After that copolymer solution was used as a liquid phase for CPC preparation and then for testing of its rheological properties. A 20% solution of PLGA-PEG-PLGA in a colloidal solution of Selenium was prepared in the same way.

4.3.3 Preparation of PLGA-PEG-PLGA/CP Composites

Alpha tricalcium phosphate (α -TCP) and monocalcium phosphate (MCP) used as powder phase (see Fig. 14) were mixed with 20% copolymer aqueous solution (see Fig. 15) with liquid to powder ratio (L/P) equal to 0.5. The mixture was stirred for 1 minute into homogenous slush structure. After that it was dosed into the syringe and transferred into Peltier system for rheology analysis.

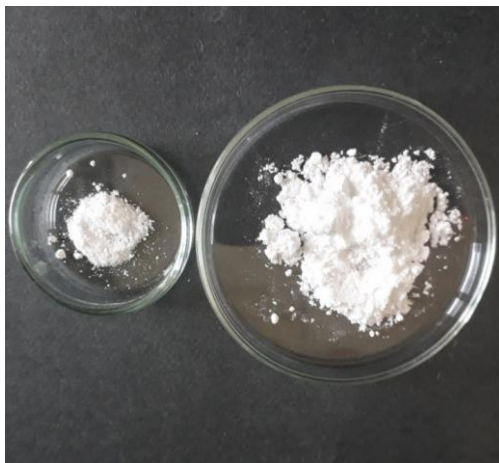


Fig. 14: Calcium phosphate ceramics. MCP and α -TCP (from left side).



Fig. 15: 20% PLGA-PEG-PLGA copolymer solution.

4.3.4 Preparation of PLGA-PEG-PLGA/DOPA/CP Composites

20% aqueous solution of the copolymer was mixed with tris(hydroxymethyl)aminoethane (TRIS) and dopamine and stirred for 30 second. Subsequently, it was mixed with the powder

phase (mixture of α -TCP and MCP) and mixed for 1 min. The mixture was stirred for 1 minute into homogenous slush structure. After that it was dosed into the syringe and transferred into Peltier system for rheology analysis.

4.3.5 Preparation of PLGA-PEG-PLGA/DOPA/NaIO₃/CP Composites

20% aqueous solution of the copolymer was mixed with TRIS and dopamine and stirred for 30 second. Subsequently, it was mixed with the powder phase (mixture of α -TCP, MCP and sodium iodate NaIO₃) and mixed for 1 min. The mixture was stirred for 1 minute into homogenous slush structure. After that it was dosed into the syringe and transferred into Peltier system for rheology analysis.

4.4 Characterization

4.4.1 Proton Nuclear Magnetic Resonance Spectroscopy

Molecular weight and polymer characterization results were confirmed using proton nuclear magnetic resonance ¹H NMR spectroscopy on 700 MHz Bruker AVANCE III HD instrument using 128 scans in deuterated chloroform (CDCl₃) solvent at 25 °C. Chemical shifts were reported in ppm relative to tetramethylsilane (TMS). ¹H NMR spectra were evaluated using ACD/1D NMR Processor.

4.4.2 Laser Particle Sizer Analyzer

The particle size distribution and mean particle size distribution of the α -TCP and MCP powder were analyzed using Laser Particle Size Analyzer LA 950 Horiba. Distilled water was used as a dispersion medium for α -TCP and MCP was dispersed in ethanol. After partial dispersion the samples were ultrasonicated for 30 minute and then measured.

4.4.3 Dynamic Light Scattering

The solution of selenium nanoparticles (SeNPs) was analysed by dynamic light scattering (DLS) method. It was ten times diluted and analysed using DynaPro NanoStar – Wyatt Technology. Two measurements were made. For DynaPro NanoStar instrument, the acquisition time was 5 seconds, the number of acquisitions per 1 measurement was 15. The temperature was 25 °C and laser was used about 663 nm.

4.4.4 Scanning Electron Microscopy

SEM MIRA 3 TESCAN was used for characterization of structure and morphology of α -TCP and MCP powder. The powder sample were performed on the carbon tape and coated with gold/palladium before testing. Accelerating voltage (10 kV), beam intensity 10 and working distance (15 mm) were used.

4.4.5 Dynamic Rheological Analyses

Rheometer AR-G2 TA instruments was used for rheological properties analysis.

4.4.5.1 CPC Rheological Analyses

The rheological properties of CPC were analysed in a dynamic stress-controlled. Plate - plate geometry with diameter 20 mm and was used for measurement. 500 μ l of CPC sample tempered to laboratory temperature was transferred to the Peltier by syringe. Rheometer was prepared to the working position (geometry gap 500 μ m). It was important to use solvent trap

filled with oil before each measurement as prevention for evaporation of the sample solvent (see Fig. 16). The experiments were carried out under the following conditions: angular frequency 1 Hz, strain 0.01% and temperature 23 °C and 37 °C.

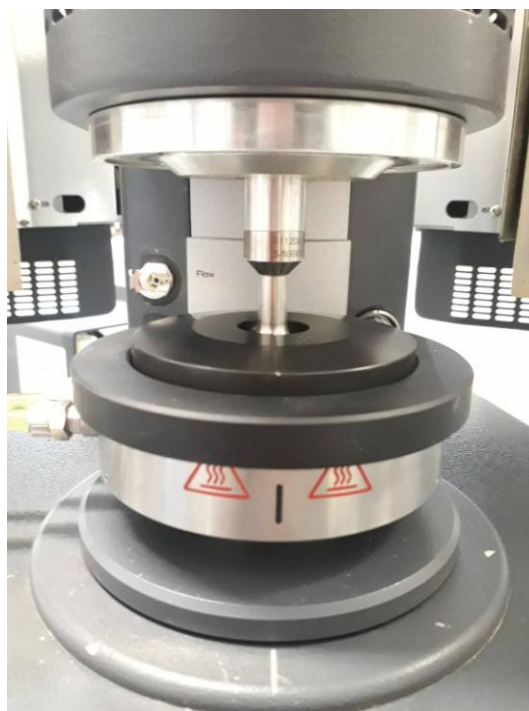


Fig. 16: Rotational rheometer with solvent trap prepared for measurement.

4.4.5.2 PLGA-PEG-PLGA Rheological Analyses

Cone-plate geometry with diameter 40 mm and 2° angle was used for temperature dependence measurement of PLGA-PEG-PLGA triblock copolymer solution. 600 µl of copolymer solution was transferred to the Peltier by spatula. After that, working position was set (geometry gap 60 µm). It was important to use solvent trap filled with water before each measurement as a prevention for evaporation of the sample solvent. The experiments were carried out under constant frequency of 1 rad·s⁻¹ and 1% strain. The temperature ramp was set from 15 to 60 °C and rate 0.5 °C per minute.

4.4.6 Steady State Rheological Analyses

For steady state rheological analyses Parallel Plate geometry with diameter 20 mm and was used for measurement. CPC sample tempered to laboratory temperature was transferred to the Peltier by syringe. Rheometer was prepared to the working position (geometry gap 500 µm). It was important to use solvent trap filled with oil before each measurement as prevention for evaporation of the sample solvent. The experiments were carried out under the following conditions: 1s⁻¹ $\xrightarrow{20s}$ 100s⁻¹ $\xrightarrow{20s}$ 1s⁻¹ and temperature was set on 23 °C. Each sample was measured at least free times.

5.1.2 Rheological Properties Characterization

Using rheological analysis were confirmed assumptions about the superior properties of PLGA-PEG-PLGA copolymer. Because of its amphiphilic character, the copolymer chains have the ability to form micelles and gel in the aqueous medium at physiological temperature. The copolymer undergoes two transitions. In case of rheological analysis, the first transition (sol-gel) is defined by gelation temperature. Gelation temperature was characterized by intersection of G' and G'' . The storage modulus became greater than loss modulus. The second intersection of G' and G'' is caused by rapid decline of G' below G'' . The gel structure begins to collapse and material loss its viscoelastic properties. This phenomenon is shown in Fig. 18. The rheological behaviour of a 20% aqueous solution of PLGA-PEG-PLGA copolymer at a temperature range of 15-60 °C was analysed. The figure shows that the first crossing occurs at a temperature of 33.7 °C. At this temperature, a sol-gel transition occurs. The second crossing, the end of the gelation, occurs at 42.5 °C. This confirms the thermosensitivity of the PLGA-PEG-PLGA copolymer and its ability to gel under the physiological conditions at given concentration (see Fig. 19). Based on the result, the 20% solution was further used for CPC preparation.

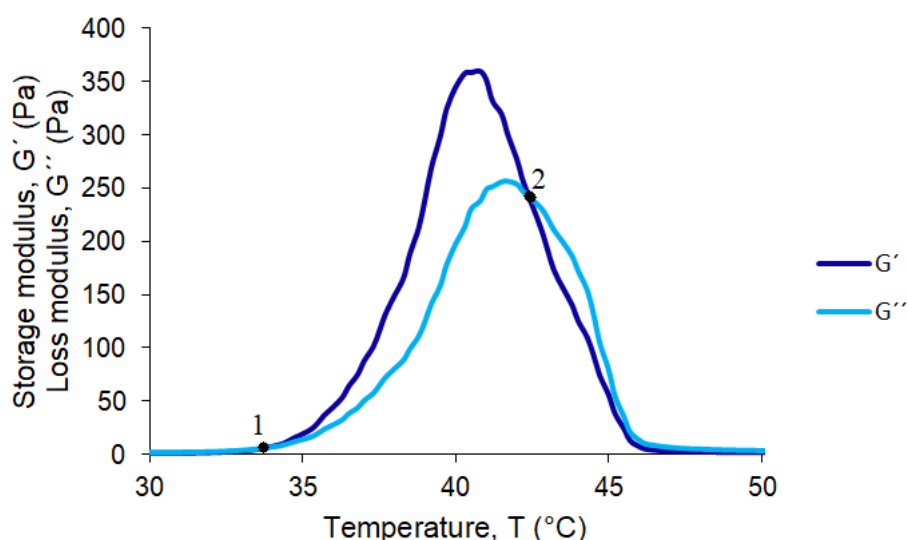


Fig. 18: Temperature dependence of 20% PLGA-PEG-PLGA aqueous solution, where 1 is sol-gel transition and 2 is the end of gelation.

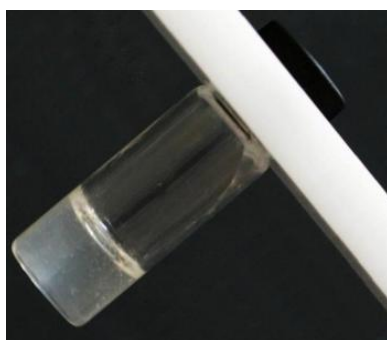


Fig. 19: 20% PLGA-PEG-PLGA copolymer at gel phase.

Rheological measurement has also been shown to demonstrate thixotropic behaviour of PLGA-PEG-PLGA copolymer. This means that the shear stress increases with the increasing shear rate and the viscosity decreases and vice versa. As can be seen in Fig. 20, the result of the measurement was a hysteresis loop confirming thixotropic behaviour gradient. Shear rate versus viscosity is shown in Fig. 21.

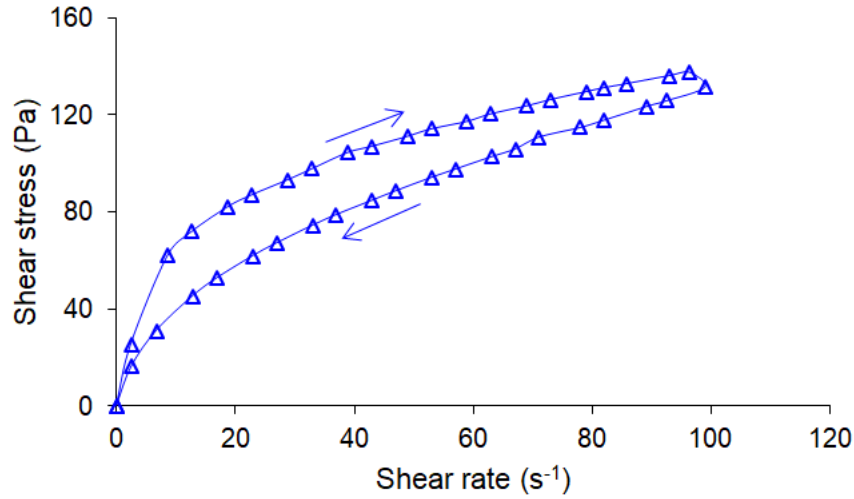


Fig. 20: Hysteresis loop as a characterisation of PLGA-PEG-PLGA thixotropy.

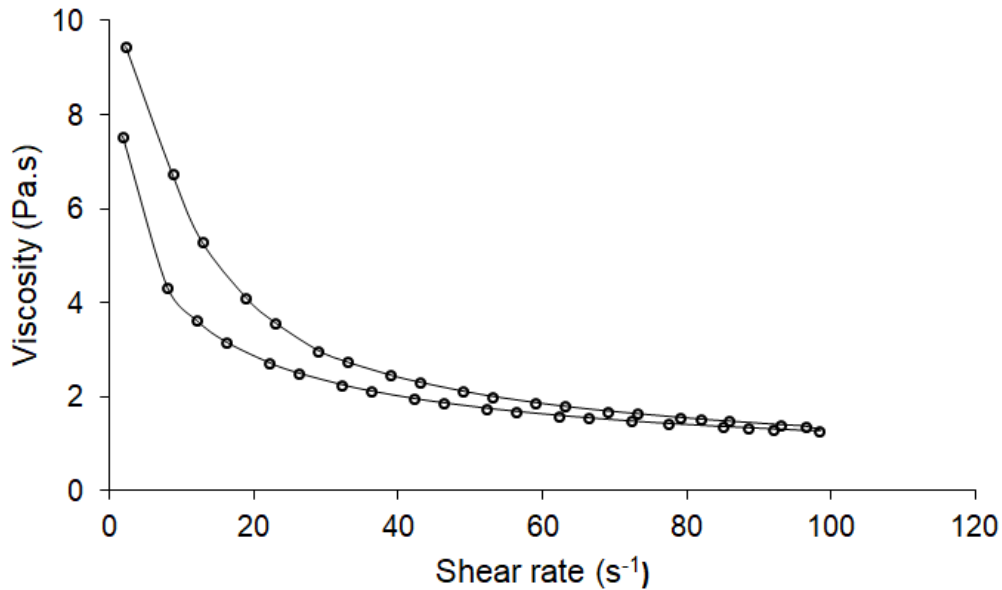


Fig. 21: Viscosity versus shear rate of 20% PLGA-PEG-PLGA copolymer.

5.2 Calcium Phosphate Powder Analysis

For the preparation of calcium phosphate cements, alpha-tricalcium phosphate (α -TCP) and monocalcium phosphate (MCP) were used. Their morphology and particle size were characterized. For these purposes, scanning electron microscopy (SEM) and laser particle size analyser were selected. As can be seen in Fig. 22b, the α -TCP particles have a spherical shape. Fig. 22a shows relatively narrow particle distribution where the mean particle size corresponds to 6.3 μm .

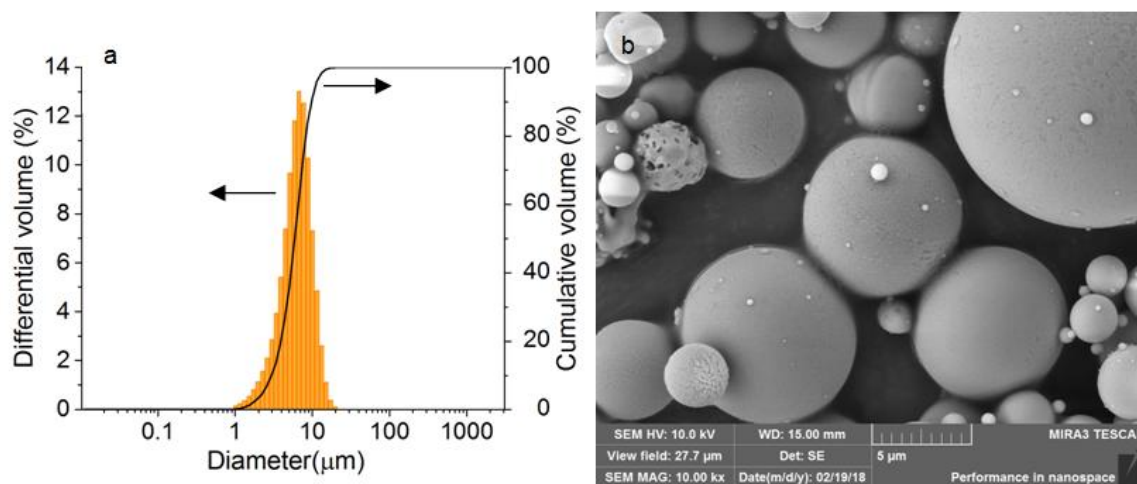


Fig. 22: a) α -TCP particle size distribution. b) SEM micrograph of α -TCP.

In the case of MCP, the particle distribution is broad and the mean particle size corresponds to 51.5 μm . It can be seen from Fig. 23a that the distribution curve has a bimodal character. The reasons are agglomerates and non-isometric particles, which were confirmed by the SEM (see Fig. 23b). Due to the morphology of MCP particles, it can be concluded that MCP will exhibit better and faster aqueous solubility than α -TCP. Based on these results, MCP was used in small amounts for faster solubility as an addition to α -TCP for CPC preparation.

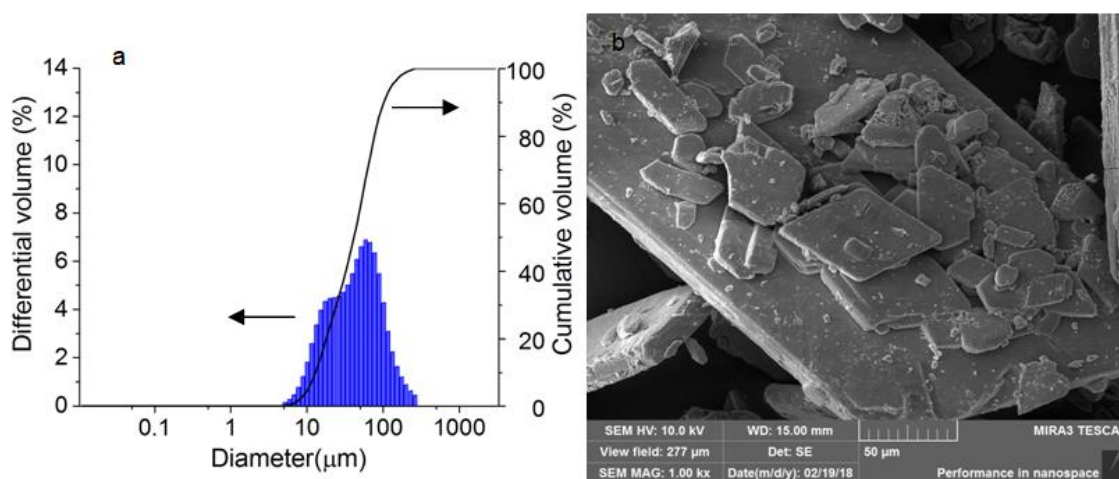


Fig. 23: a) MCP particle size distribution. b) SEM micrograph of MCP.

5.3 Selenium Nanoparticles Analysis

Selenium nanoparticles were characterized by SEM and Dynamic light scattering method (DLS). Fig. 24b shows the spherical shape of selenium nanoparticles. The mean diameter of nanoparticles is 136 nm shown in Fig. 24a, however, there are as well nanoparticles about 12 nm in size.

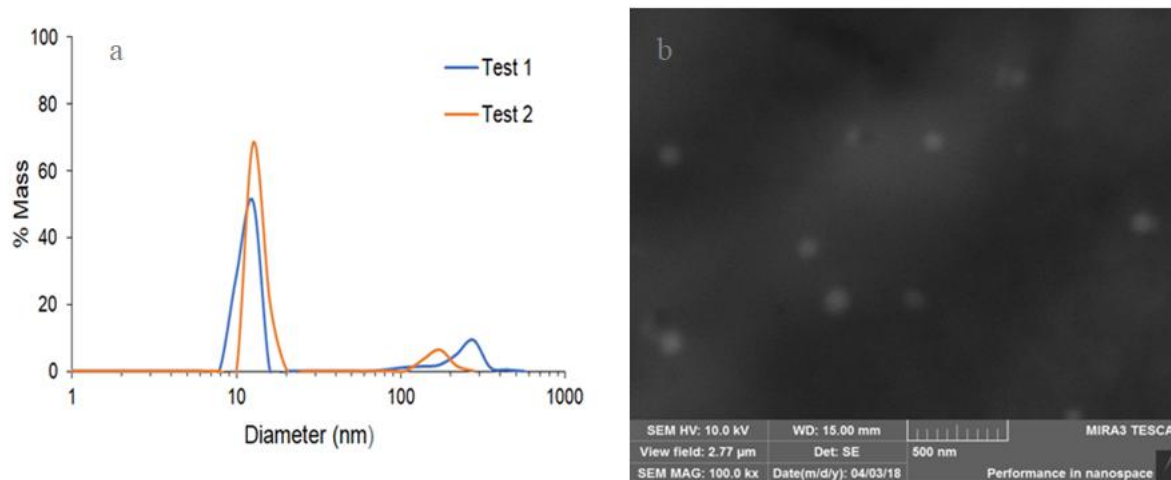


Fig. 24: a) particle size distribution and b) SEM micrograph of selenium nanoparticles.

5.4 Rheological Behavior of Modified PLGA-PEG-PLGA/CP Pastes

Rheological analysis allowed to monitor the process of self-setting reaction of calcium phosphate bone cements under the given temperature conditions (23 to 37 °C). The measurements also provided valuable information about the thixotropic behavior of the pastes. The linear viscoelastic region was analysed by measurement of frequency and strain sweep. The list of samples and their composition studied in this work is given in Tab. 5. The sample composed of 20% PLGA-PEG-PLGA, MCP and α -TCP (20% ABA + MCP + α -TCP) was used as a reference.

Tab. 5: Summary of analysed samples, their composition and visual characteristics.

Sample	Composition	L/P	pH	Visual characteristics
ABA+C	Liquid: 20% ABA	0.5	7.3	White
	Powder: 2 % MCP, 98 % α -TCP			
ABA+C+D	Liquid: 20% ABA, Dopamine	0.5	7.9	Slightly grey after mixing
	Powder: 2 % MCP, 98 % α -TCP			
ABA+C+D+I	Liquid: 20% ABA, Dopamine	0.5	7.6	Slightly pink after mixing, dark grey after setting
	Powder: 2 % MCP, 98 % α -TCP, Sodium Iodate			
W+C	Liquid: Ultra pure water	0.5	-	White and the most viscous
	Powder: 2 % MCP, 98 % α -TCP			
ABA+C+SeNPs	Liquid: 20% ABA in colloid solution of SeNPs	0.5	-	Slightly orange
	Powder: 2 % MCP, 98 % α -TCP			

ABA = PLGA-PEG-PLGA, C = powder phase composed of MCP and α -TCP, D = dopamine, I = Sodium Iodate, W = ultra pure water, SeNPs = selenium nanoparticles

5.4.1 Measurement Optimization

Before the start of measurement, it was necessary to optimize the rheological analysis method. Immediately after mixing liquid and powder, a hydrolytic reaction occurs. For this reason, it was important to carefully set up and follow the sampling procedure. It was desirable that the sample be sufficiently mixed into a homogeneous paste form. After previous experience of the research group of assoc. prof. Vojtová, sample was mixed exactly one minute. Subsequently, it was dosed and analysed at the latest within 3 minutes after mixing. The sample was originally dosed with spatula. However, the spatula did not provide exact volume dosing. Therefore, syringe dosing has been selected. It was also necessary to prevent evaporation of the solvent during the measurement. This was achieved through the use of solvent trap. In the previous study of CPC pastes, water was added to a solvent trap. During the measurement, which took place over a longer time period at higher temperatures, water tend to be evaporated and causing subsequent drying and distortion of the results. Two options were offered as a solution. Add water to the reservoir during measurement or choose another temperature-stable liquid. Water replenishment is a less convenient solution that requires thorough setup. It was necessary to add water with thought. The reservoir is very small and when a slightly larger volume of water has been added, the sample was "flooded" and thus influenced the measurement. Due to this, the second and more convenient option was taken. The solvent trap was filled with oil which exhibited better thermal stability. To ensure reproducible measurement was necessary to strictly follow these conditions.

5.4.2 Steady Rheological Properties of Modified CPC

Steady rheological behavior was studied in all the samples listed in Tab. 5. It is a dependence of the shear velocity on the shear stress. Steady rheological behavior was characterized by shear rates ranging from 1 to 100 s^{-1} up ($1s^{-1} \xrightarrow{20s} 100s^{-1}$) and down ($100s^{-1} \xrightarrow{20s} 1s^{-1}$). The measurement was started 2 minutes after careful mixing of the paste.

Fig. 25 shows the shear rate dependence on the shear stress of three samples (ABA, W + C and ABA + C). In the case of samples C + W + C and ABA, different type of liquid phase was used. In all cases, there are hysteresis loops indicating thixotropic behavior. The direction of the curves subsequently points to positive thixotropy.

For a paste containing water as a liquid phase, at first it is necessary to exceed the high shear stress compared to the paste containing a 20% aqueous solution of a PLGA-PEG-PLGA copolymer. Thixotropy affects injectability. The paste W + C was less injectable and did not hold well in shape and showed a tendency of phase separation. On the other hand, the ABA + C paste containing the copolymer solution was stronger, held in shape and exhibited no phase separation. It was very well injectable and there was no need to overcome the higher shear stress as in the W + C sample. This can also be observed from the curve. For the comparison of thixotropic properties, a curve characterizing this type of behavior of the aqueous solution of PLGA-PEG-PLGA copolymer alone was plotted in the graph. For this sample, it is clear that there is no need to overcome such a high shear stress as the CPC past.

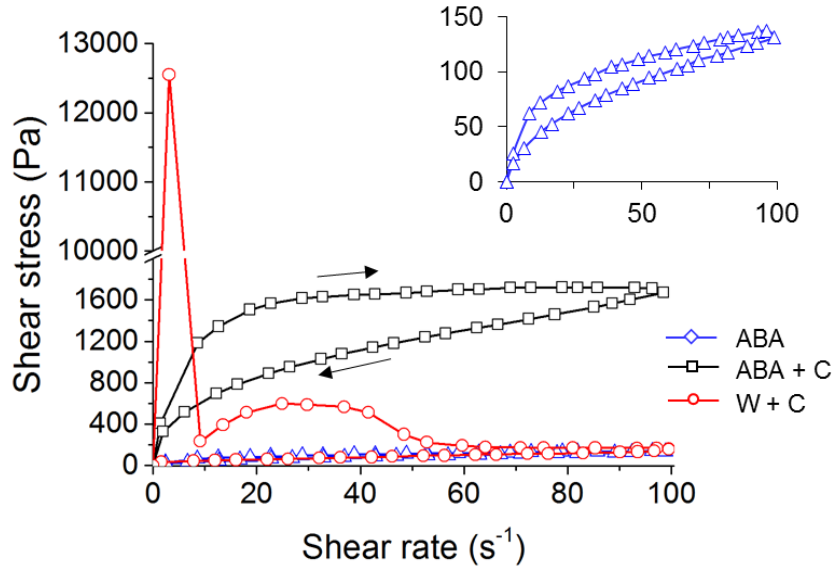


Fig. 25: The relationship between shear stress and shear rate of samples W+C, ABA and ABA+C measured in range of shear rates from 1 to 100 s^{-1} .

Fig. 27 shows the relationship between viscosity and shear rate. From the plot, the tendency is observed when the viscosity decreases with the increasing shear rate, or the viscosity increases with decreasing shear rate. This also points to the thixotropic behavior of CPC. For the W + C paste, it can be observed that the initial viscosity is very high and with a rising shear rate it drops very rapidly at increasing shear rates. Subsequently, when the rate was reduced, the viscosity increased only slightly. This could be due to the poor consistency of the paste. Due to high shear stress, the paste tended to form a very dense cluster compared to a paste containing a 20% solution of the copolymer, which remained homogeneous throughout the experiment and throughout the shear rate range (see Fig. 26).

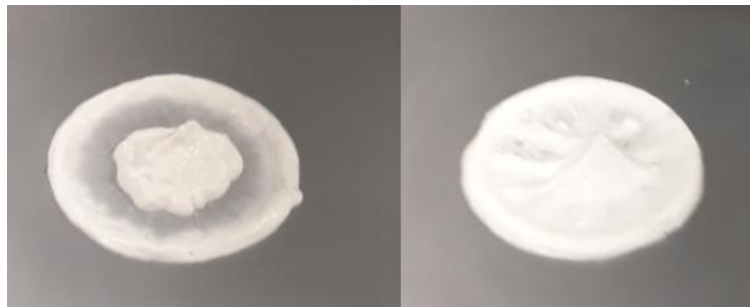


Fig. 26: The samples after steady state rheological measurement. The shear rate range from 1 to 100 % upward and from 100 to 1 % downward. From the left side: W+C, ABA+C.

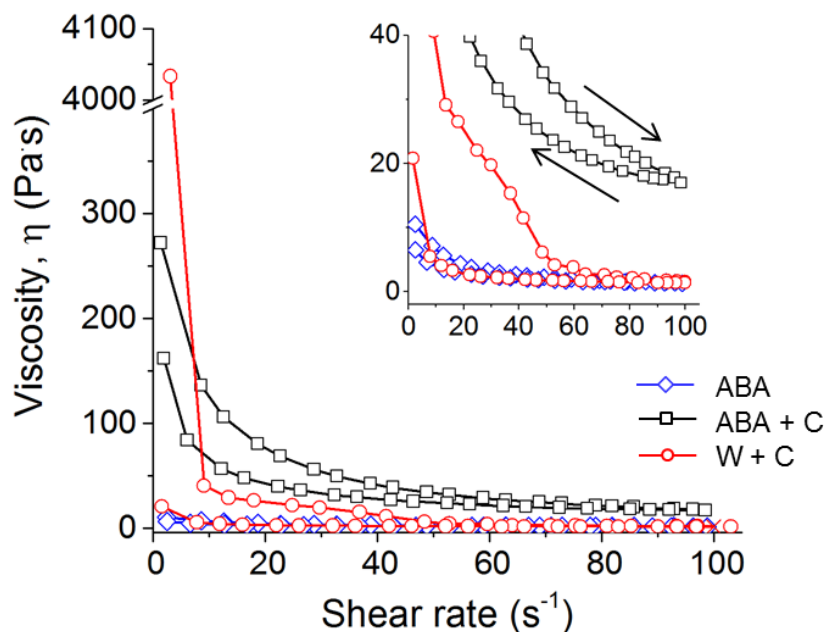


Fig. 27: Viscosity versus shear rate upward and downward flow paths at 23 °C. Samples: ABA, ABA+C, W+C.

Bone paste (ABA + C) was modified with dopamine (ABA + C + D), which has the ability to polymerize in an aqueous environment to form polydopamine. Polydopamine can be further networked. Sodium iodate was used as a crosslinker and added to the paste in small amounts (ABA + C + D + I). From Fig. 28 it is clear that dopamine did not affect the thixotropic behavior of the CPC. This is due to the fact that the paste was measured relatively briefly after mixing, which could have led to insufficient dopamine polymerization and its effect on the paste behavior was not enough.

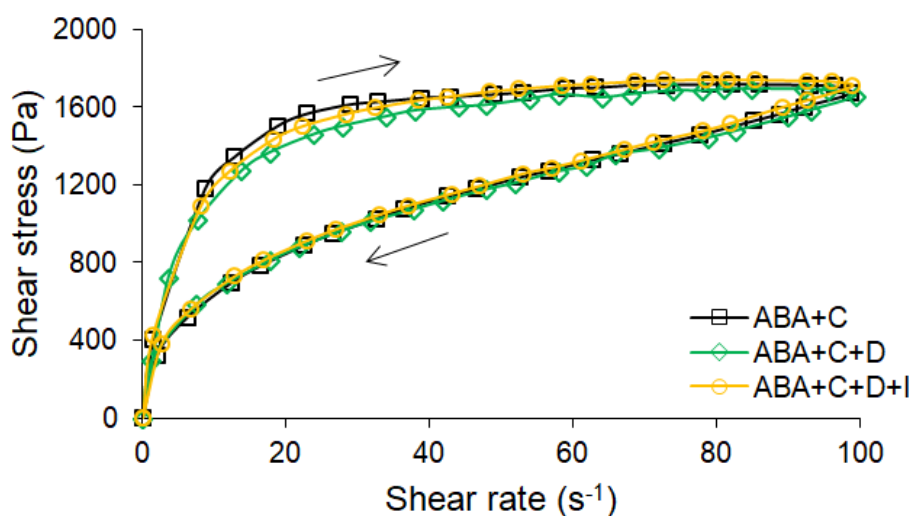


Fig. 28: The relationship between shear stress and shear rate of samples ABA+C, ABA+C+D and ABA+C+D+I measured in range of shear rates from 1 to 100 s⁻¹.

It would be better to measure later than 2 minutes after mixing and dopamine polymerization would take place, the effect of these additives on thixotropy could be more apparent. It is clear that even the addition of the crosslinker will not have an effect on thixotropy under the given conditions (see Fig. 28). Sodium iodate acts as a crosslinker only in the presence of polydopamine chains. This fact can be verified in the future by studying the thixotropic behavior of the paste for longer periods of time after mixing. A plot showing the viscosity versus shear rate is shown in Fig. 29. From the plot, it can be observed that, as in the previous case, the viscosity decrease sharply at lower shear rates (approximately up to 30 s^{-1}). At higher speeds, there is a slight decrease.

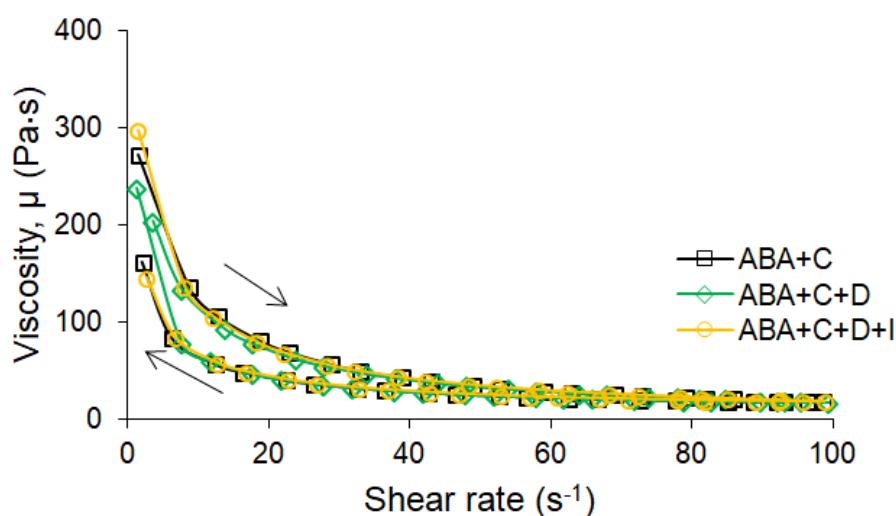


Fig. 29: Viscosity versus shear rate upward and downward flow paths at $23\text{ }^{\circ}\text{C}$. Samples: ABA+C, ABA+C+D, ABA+C+D+I.

CPC was also modified with additional selenium nanoparticles in colloidal chitosan solution. The principle was to dissolve PLGA-PEG-PLGA copolymer directly in the selenium nanoparticle (SeNPs) colloid solution. The solution was then mixed with a powder phase of the same composition as in the previous pastes. The reason for the addition of SeNPs was to improve the antibacterial properties of CPC. Rheological analysis was performed to verify that SeNPs will not have a negative effect on rheological properties of the pastes. The interesting finding was that the addition of SeNPs affected the thixotropic behavior of the paste. It is evident from Fig. 30 that the ABA + SeNPs + C paste is more thixotropic than the ABA + C paste. Likewise, it has a higher initial viscosity than ABA + C (see Fig. 31). The reason for this is the addition of nanoparticles. The influence of nanoparticle addition on the rheological properties of the systems has been the subject of many studies. Studies show that nanoparticles in colloidal solutions can interact (Brownian motion). Higher friction may occur and therefore decrease in viscosity. Hence, if material has higher shear rates, Brownian motion will be negligible and viscosity will decrease. This is also the reason why, at higher shear rates, the viscosities of both pastes were evenly balanced, although the ABA + SeNPs + C paste was initially more viscous.

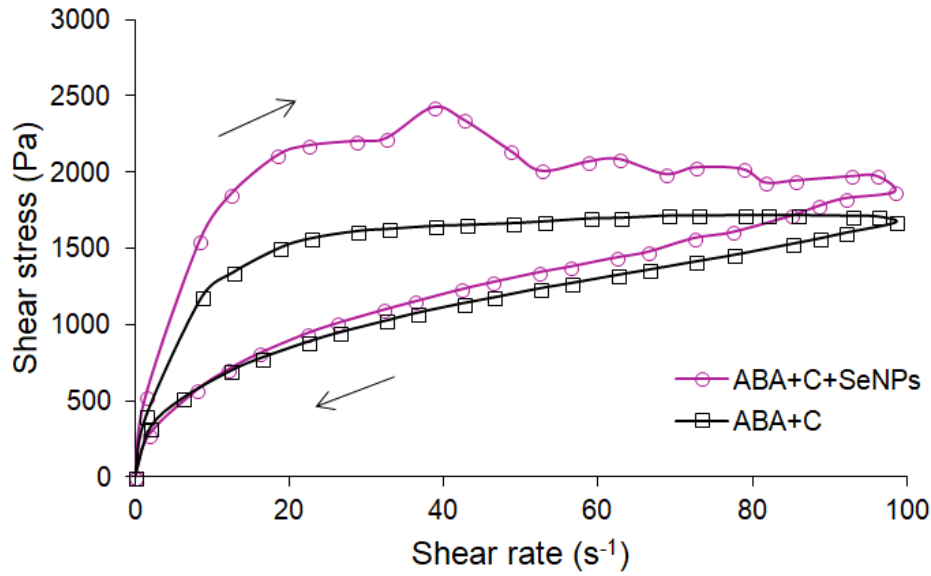


Fig. 30: The relationship between shear stress and shear rate of samples ABA+C+SeNPs and ABA+C measured in range of shear rates from 1 to 100 s^{-1} .

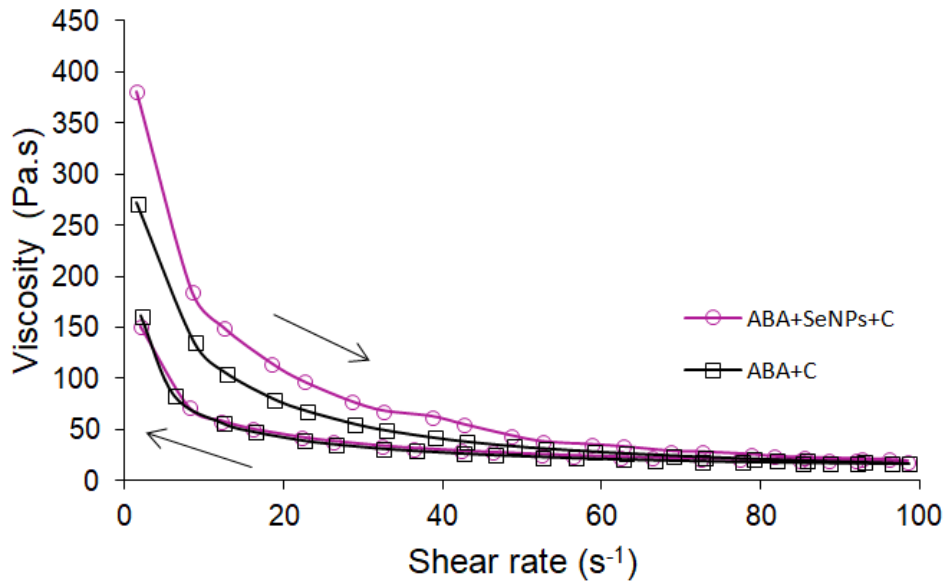


Fig. 31: Viscosity versus shear rate upward and downward flow paths at 23 °C. Samples: ABA+C, ABA+SeNPs+C.

As mentioned above, thixotropic curves are an important factor in characterizing the stability of pastes. The larger the area of the thixotropic loop, the more stable the paste is. This means that there is no sedimentation, phase separation. The paste is homogeneous and holds the shape. From these thixotropic curves, the area sizes between the curves were calculated. The material thixotropy can be quantified by thixotropic loop area calculation. It is also true that the greater the thixotropy, the greater the energy is needed to break down the thixotropic structure. The calculated values were plotted in Fig. 32. One can say that lowest thixotropy was founded in case of 20% ABA. Pastes like ABA + C, ABA + C + D, ABA + C + D + I and W + C exhibit comparable thixotropy size. Compared to ABA, it is larger, which means a

more stable paste. The exception is W + C. Although the thixotropy size is comparable to the mentioned pastes, it differs in the course of thixotropic behavior, as explained above. As a result, an important parameter is not only the size of the surface but also the behavior of the material depending on the shear velocity. The most thixotropic was SeNPs+ABA+C paste. This means that it is the most stable paste.

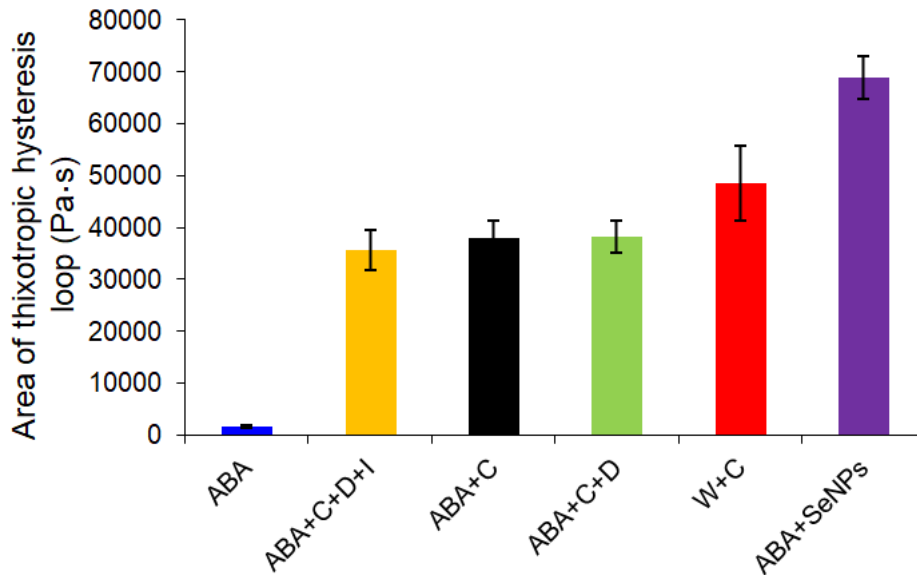


Fig. 32: Calculated values of area of thixotropic hysteresis loop for all studied modified pastes.

5.4.3 Linear Viscoelastic Region

For time sweep measurement, it was necessary to set appropriate parameters such as strain (stress) and frequency. It was desirable that the selected values were in the linear viscoelastic region (LVR) where storage modulus (G') and loss modulus (G'') are not dependent on the strain or frequency. The sample 20% ABA+ceramics were used for LVR analysis.

5.4.3.1 Strain Sweep

The measurement was carried out at changing strain amplitudes in the range of 0.001-500 %, constant frequency 1 Hz and temperatures 23 and 37 °C. From Fig. 33 it can be seen that the temperature did not have a significant effect on the linear viscoelasticity region. Temperature affected mainly the elastic modulus of the sample. The intersection of G' and G'' occurred at higher values of strain at 37 °C, than at 23 °C. This was due to the phase transition of the PLGA-PEG-PLGA solution at this temperature, thereby obtaining a gel structure. LVR is defined by the constant dynamic moduli G' and G'' . The graphs show that LVR is a relatively small in region of very low strain values. At the point where it ends LVR, there has been a gradual decline in the module. For this reason, the value of 0.01 %, which was used to investigate frequency sweep, was selected.

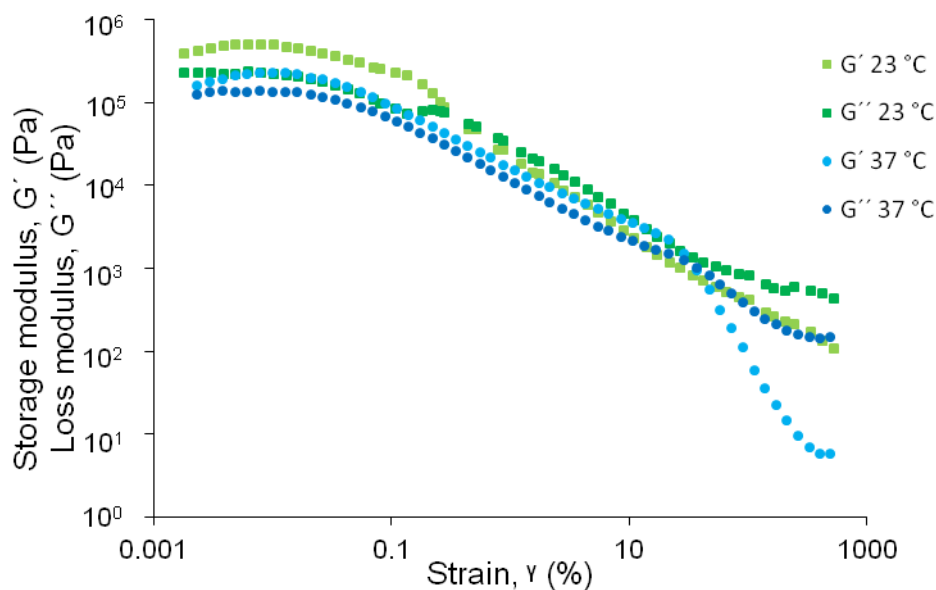


Fig. 33: Dynamic moduli of ABA+C sample at constant frequency (1 Hz), temperature 23 and 37 °C and changing strain at the range of 0.001-500 %.

5.4.3.2 Frequency Sweep

To determine the LVR in which the module is independent of the applied frequency, a sample of the basic composition (ABA+C) was analysed. Experiments were carried out at 23 and 37 °C, 0.01% strain and frequency range between 0.16-16 Hz (1-100 rad·s⁻¹). In case of frequency sweep, the temperature effect is visible. Both G' and G'' are relatively constant at 23 °C (see Fig. 34). However, it very slightly increases at higher values of frequency. On the other hand the loss modulus is higher at low frequency at 37 °C. It is caused by gelation of PLGA-PEG-PLGA solution. The beginning of gelation is defined by intersection of G' and G'' where $G' = G''$. Although the PLGA-PEG-PLGA solution gels at 37 °C, the intersection of G' and G'' appeared approximately more than one minute after the measurement beginning. Due to the hydrolysis of CPC, it was not advisable to keep the sample for longer to temper. The frequency was set on 1 Hz for other experiment.

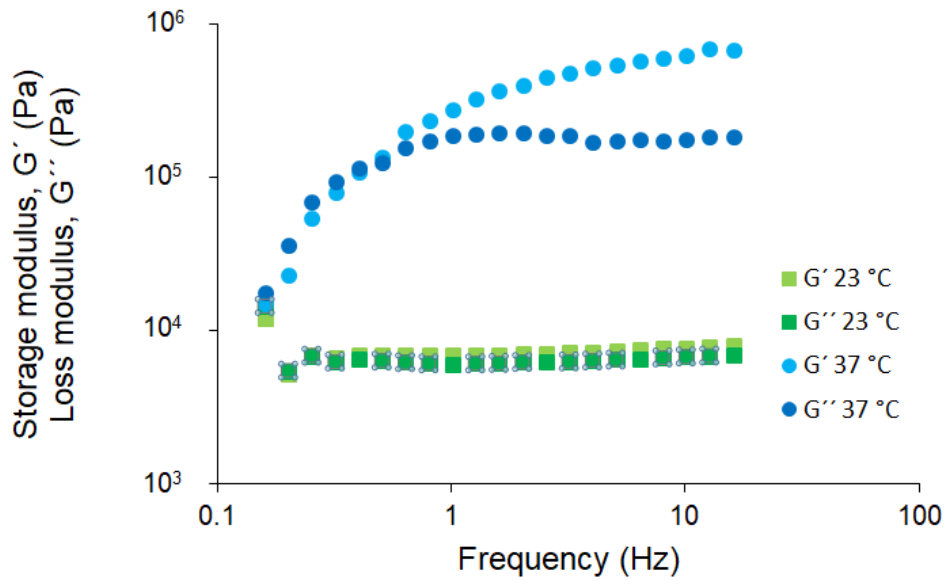


Fig. 34: Dynamic moduli of ABA+C sample at constant strain (0.01 %), temperature 23 and 37 °C and changing frequency at the range of 0.16-16 Hz.

It is evident from Fig. 35 that complex viscosity decreases with increasing frequency, indicating that CPC is a non-Newtonian system exhibiting shear thickening.

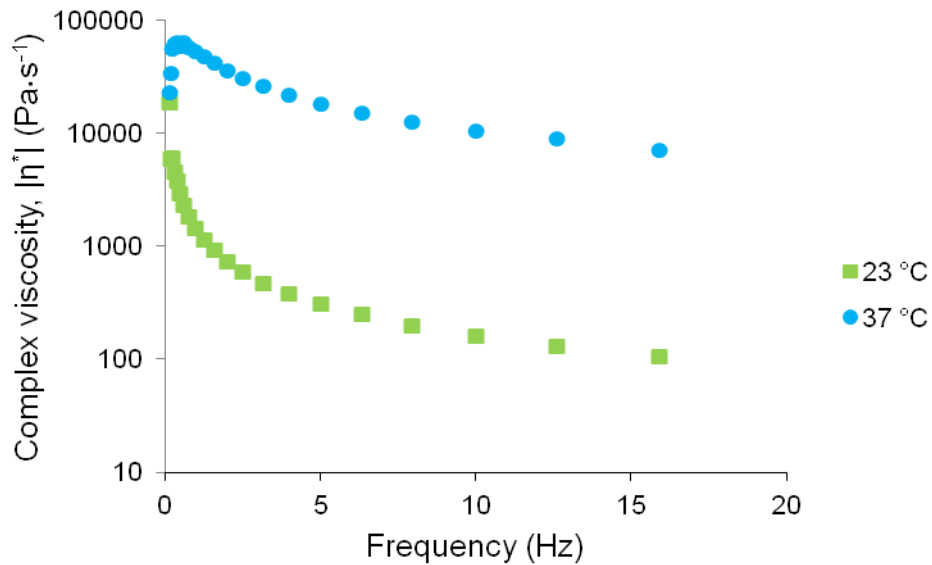


Fig. 35: The relationship between complex viscosity and applied frequency range 0.16-16 Hz.

5.4.4 Time Sweep Response

A dynamic time sweep was used to observe the CPC setting process. Measurements were performed at frequency of 1 Hz and at very low strain rate of 0.01%. The curing process was monitored at 23 °C (room temperature) and 37 °C (physiological condition). Figure Fig. 36 shows a time sweep responses of G' , G'' and η^* . It is obvious that G' , G'' and η^* grow with increasing time. At the beginning the intersection of G' and G'' is observed. The reason is the phase transition of the PLGA-PEG-PLGA solution to the gel structure. Setting process is

based on the principle of dissolution and precipitation. The fastest is to dissolve (hydrolyze) MCP, then α -TCP. The final product, which is calcium deficient hydroxyapatite (CDHA) starts to form by precipitation reaction.

Curves (see Fig. 36) can be divided into two sections. The first section started with low values of modulus that is slowly increasing. The second section began after approximately 50 minutes, it can be observed that the modules started to increas noticeably and the paste began to cure quickly. Since all three variables (G' , G'' and η^*) have the same behavior over time, G' was chosen to describe the modified CPC setting process. Time sweep response at 26 °C showed the same trend also for all three variables.

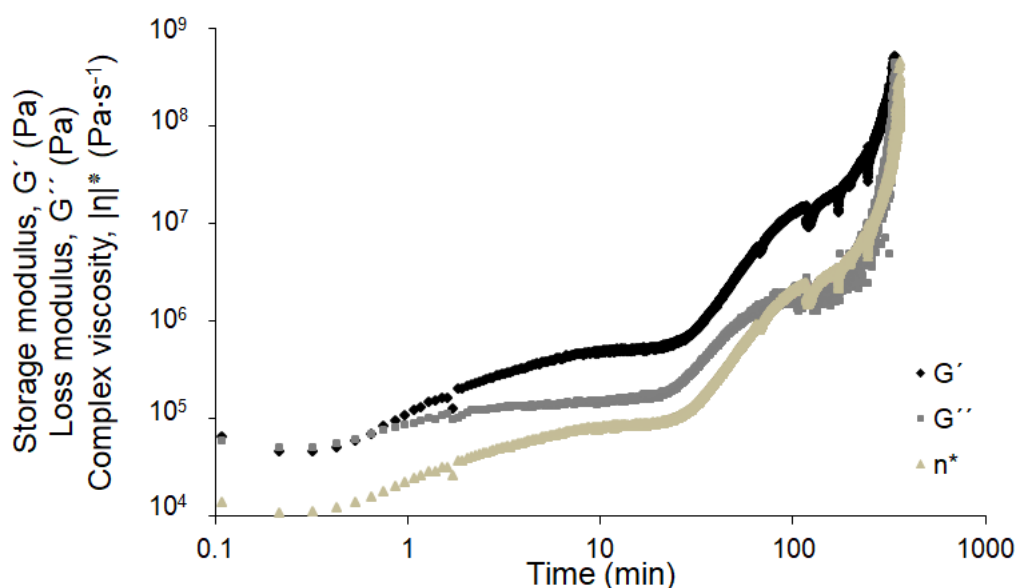


Fig. 36: Time sweep response of G' , G'' and η^* of ABA+C at 37 °C. Parameters of measurement: frequency 1 Hz, strain 0.01 %.

Fig. 37 shows the dependence G' with the time at 26 °C. The measurement was carried out for 3 hours. The aim was to find the approximate processing time of the paste. Respectively, the time after which the paste begins to cure. "Processing time" means the time during which the paste is still injectable and capable of being applied. For accurate determination of the cure time, the Vicat method would have to be performed. However, dynamic rheological analysis is also able to provide the approximate setting time.

One can say that the dopamine modified paste (ABA+C+D) is the fastest. As mentioned above dopamine is able to polymerize in aqueous solution at higher pH. pH was adjusted by adding of TRIS. However the reaction occurs at basic environment, pH of modified pastes was only slightly above 7. Addition of sodium iodate caused later setting (sample ABA+C+D+I). Sodium iodate is a weak nucleophile capable of crosslinking polydopamine chains. This means that dopamine polymerization must first occur and then it is cross-linked. After cross-linking very rapid setting occurred and G' started to rise sharply.

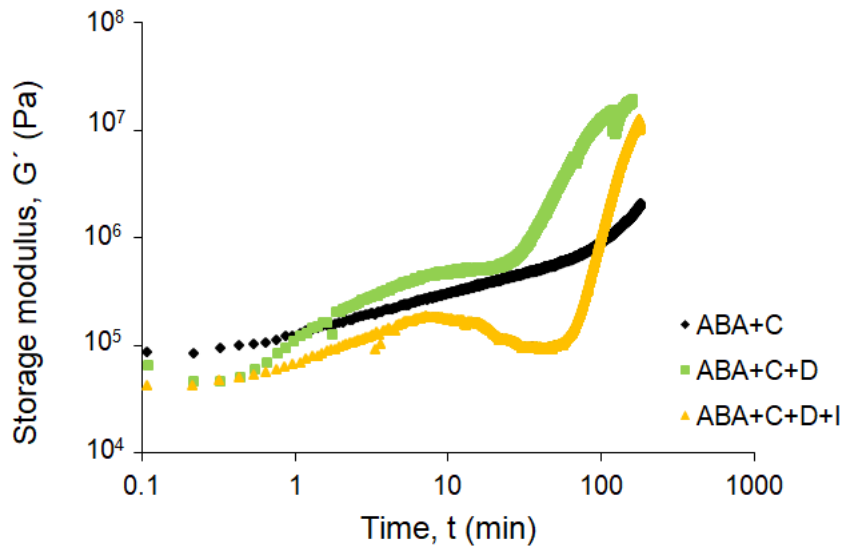


Fig. 37: Time sweep response of G' of ABA+C, ABA+C+D and ABA+C+D+I at 23 °C. Parameters of measurement: frequency 1 Hz, strain 0.01 %.

The slowest setting showed the paste without the additives. G' was continuously but slowly increased. In about 100 minutes, there is a hint that at about this time G' started to increase faster.

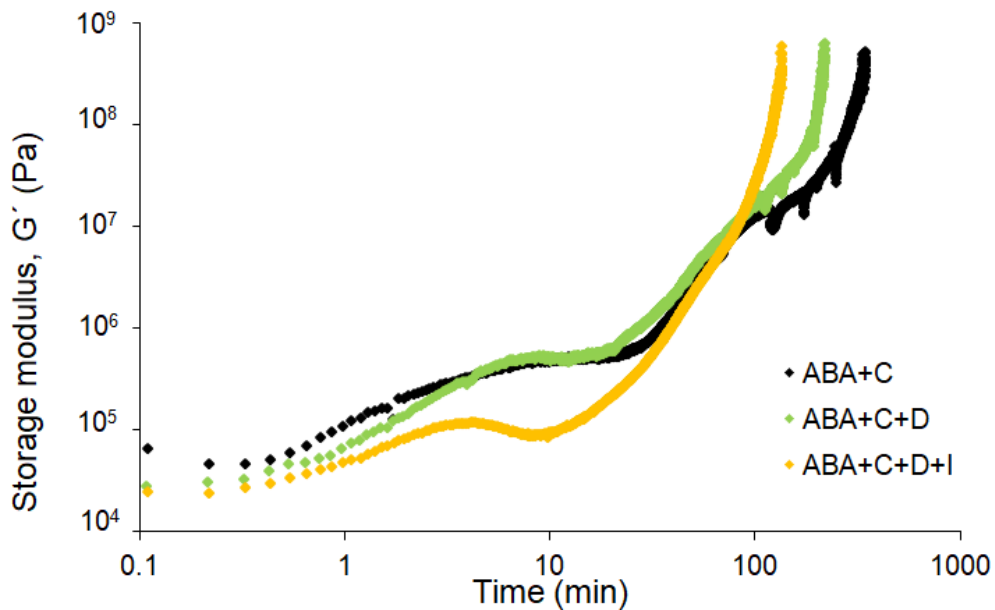


Fig. 38: Time sweep response of G' of ABA+C, ABA+C+D and ABA+C+D+I at 37 °C. Parameters of measurement: frequency 1 Hz, strain 0.01 %.

Fig. 38 shows the setting during physiological conditions (37 °). Paste ABA+C+D+I showed at the beginning the lowest module, which increased very slowly in comparison to other pastes. Still, the setting of this paste was the fastest. The reason was sudden growth of G' . The setting for value in order 10^8 Pa took approximately 130 minutes. In the ABA+C+D paste, setting was slower (about 210 minutes), although the module grew faster than ABA+C+D+I. Setting

of the paste without additives took approximately 320 minutes and was the slowest. The interesting question was whether sodium iodate only acts as a crosslinker or is able to influence the behavior of the paste even without the presence of polydopamine. For this reason, the ABA+C+I composition paste (no dopamine added) was subjected to analysis. Sodium iodate alone has been found to have no effect on the rheological properties, and it really acts only as a crosslinker, since the cure time corresponded to the ABA + C paste. Thus dopamine appears to be a very suitable additive for modifying CPC to improve the rheological and mechanical properties. On the other hand, dopamine has great potential not only as an additive to improve rheological properties, but also because of its excellent adhesive properties it also promotes and improves adhesion to the bone.

The time sweep response paste modified by the addition of selenium nanoparticles (ABA + SeNPs + C) is shown in Fig. 39. Although the paste exhibited a higher modulus compared to ABA + C, the addition of SeNPs had no effect on paste curing at 23 °C. The reason of higher modulus is discussed in chapter 5.4.2. Although it should be noted that the viscosity can be greatly affected by the manner and stirring rate of pastes. This is a parameter that is heavily dependent on the human factor.

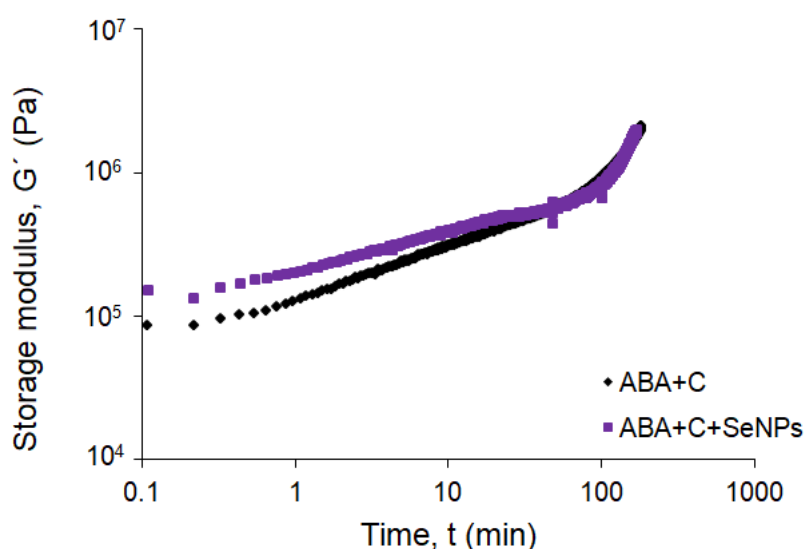


Fig. 39: Time sweep response of G' of ABA+C, ABA+SeNPs+C at 23 °C. Parameters of measurement: frequency 1 Hz, strain 0.01 %.

A very positive finding was that selenium nanoparticles affect paste setting at 37 °C (see Fig. 40). One can say that the initial course of setting corresponded to the curing time of ABA + C. However, the modulus increased much faster than ABA+C. The ABA+SeNPs+C paste was cured for approximately 230 minutes. This is very similar to the time of dopamine-modified paste setting. The reason why SeNPs provided a faster cure may be that SeNPs may also act as a nucleating agent to promote crystal formation.

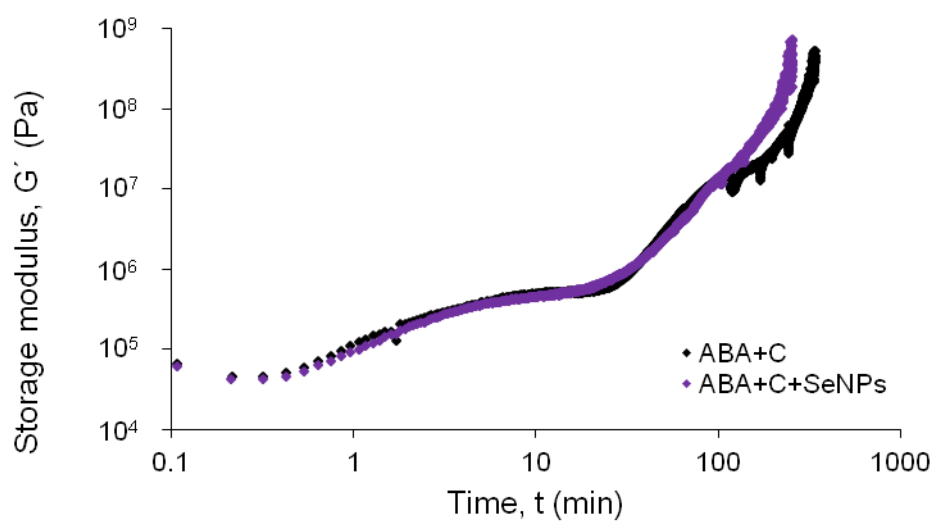


Fig. 40: Time sweep response of G' and of ABA+C, ABA+SeNPs+C at 37 °C. Parameters of measurement: frequency 1 Hz, strain 0.01 %.

6 CONCLUSION

The aim of the diploma thesis was to evaluate the rheological properties of calcium phosphate bone cement (CPC) based on thermosensitive copolymer PLGA-PEG-PLGA and calcium phosphate bioceramic by methods of dynamic rheological analysis and steady state rheological analysis. Both pastes of basic composition (ABA + C) and pastes modified by addition of dopamine, sodium iodate and selenium nanoparticles were studied. It was found that the thermosensitive copolymer contained in the liquid phase significantly influenced the thixotropic behavior of the pastes. The pastes modified by dopamine and sodium iodate did not shown any changes in thixotropic behavior compared to the base composition paste. A positive effect on thixotropy was also observed in the modified tailings by selenium nanoparticles.

The CPC setting process was also followed. On the basis of the results, one can say that the paste modified with dopamine and sodium iodate (ABA + C + D + I) showed faster setting approximately about 130 minutes. Compared to the base composition paste, the reaction accelerated by approximately 190 minutes, which is a very positive finding. In this regard, dopamine and sodium iodate, as a crosslinker, appear to be very suitable additives to improve not only the rheological properties of the pastes. Surprisingly, it was also found that the setting reaction was also affected by the addition of selenium nanoparticles by about 100 minutes. In the context of a future CPC study of this type, it would certainly be desirable and interesting to examine the rheological properties of the pastes modified by both dopamine with crosslinker and selenium nanoparticles. Interestingly, the ABA + C + D + I paste, which exhibited the fastest setting reaction, was the slowest in its initial setting. This means that it is a paste with the longest processing time.

Due to the fact that the rheological properties can be corrected with concentration, L/P ratio, or particle size, these possibilities provide additional suggestions for potential future study of the pastes focusing on improving not only mechanical but also bioactive properties.

In conclusion, all used additives have been evaluated from the rheological point of view as very suitable for use in the field of bone cement research. None of the additives were observed to have a negative effect on the properties tested.

7 REFERENCES

- [1] Barrère F, van Blitterswijk CA, de Groot K. Bone regeneration: molecular and cellular interactions with calcium phosphate ceramics. *International Journal of Nanomedicine*. 2006;1(3):317-332.
- [2] AMINI, Ami R., Cato T. LAURENCIN and Syam P. NUKAVARAPU. Bone Tissue Engineering: Recent Advances and Challenges. *Critical Reviews™ in Biomedical Engineering*. 2012, 40(5), 363-408. DOI: 10.1615/CritRevBiomedEng.v40.i5.10. ISSN 0278-940x. Available from: <http://www.dl.begellhouse.com/journals/4b27cbfc562e21b8,489cce62273b4868,20e3cde6200d53aa.html>
- [3] SLÍPKA, Jaroslav. *Základy histologie*. Praha: Karolinum, 2014. ISBN 978-80-246-2809-7.
- [4] SADAT-SHOJAI, Mehdi. Calcium Phosphate–Reinforced Polyester Nanocomposites for Bone Regeneration Applications. *Biodegradable Polymeric Nanocomposites*. CRC Press, 2015, 2015-10-16, 1-34. DOI: 10.1201/b19314-2. ISBN 978-1-4822-6051-9. Available from: <http://www.crcnetbase.com/doi/10.1201/b19314-2>
- [5] CRANE, Genevieve M., Susan L. ISHAUG and Antonios G. MIKOS. Bone tissue engineering. *Nature Medicine*. 1995, 1(12), 1322-1324. DOI: 10.1038/nm1295-1322. ISSN 1078-8956. Available from: <http://www.nature.com/doifinder/10.1038/nm1295-1322>
- [6] Transplantation and Rejection. In: Clinical Gate [online]. 2015 [cit. 2018-03-03]. Available from: <https://clinicalgate.com/transplantation-and-rejection/>
- [7] ZHANG, Jingtao, Weizhen LIU, Verena SCHNITZLER, Franck TANCRET and Jean-Michel BOULER. Calcium phosphate cements for bone substitution: Chemistry, handling and mechanical properties. *Acta Biomaterialia* [online]. 2014, 10(3), 1035-1049 [cit. 2018-03-03]. DOI: 10.1016/j.actbio.2013.11.001. ISSN 17427061. Available from: <http://linkinghub.elsevier.com/retrieve/pii/S1742706113005576>
- [8] MAAS, Michael, Ulrike HESS and Kurosch REZWAN. The contribution of rheology for designing hydroxyapatite biomaterials. *Current Opinion in Colloid & Interface Science* [online]. 2014, 19(6), 585-593 [cit. 2018-03-04]. DOI: 10.1016/j.cocis.2014.09.002. ISSN 13590294. Available from: <http://linkinghub.elsevier.com/retrieve/pii/S1359029414000892>
- [9] Bone engineering. Toronto: Em squared incorporated, 2000. ISBN 09-686-9800-X.

- [10] BRONZINO, Joseph D. The biomedical engineering handbook. 3rd ed. Boca Raton: Taylor & Francis Group, 2006. ISBN 08-493-2121-2.
- [11] KHAN, Ather Farooq, Muhammad SALEEM, Adeel AFZAL, Asghar ALI, Afsar KHAN and Abdur Rahman KHAN. Bioactive behavior of silicon substituted calcium phosphate based bioceramics for bone regeneration. *Materials Science and Engineering: C* [online]. 2014, 35, 245-252 [cit. 2018-03-03]. DOI: 10.1016/j.msec.2013.11.013. ISSN 09284931. Available from: <http://linkinghub.elsevier.com/retrieve/pii/S0928493113006267>
- [12] GINEBRA, Maria-Pau, Cristina CANAL, Montserrat ESPANOL, David PASTORINO and Edgar B. MONTUFAR. Calcium phosphate cements as drug delivery materials. *Advanced Drug Delivery Reviews* [online]. 2012, 64(12), 1090-1110 [cit. 2018-03-03]. DOI: 10.1016/j.addr.2012.01.008. ISSN 0169409X. Available from: <http://linkinghub.elsevier.com/retrieve/pii/S0169409X12000117>
- [13] O'HARA, R., F. BUCHANAN and N. DUNNE. Injectable calcium phosphate cements for spinal bone repair. *Biomaterials for Bone Regeneration* [online]. Elsevier, 2014, 2014, s. 26-61 [cit. 2018-03-03]. DOI: 10.1533/9780857098104.1.26. ISBN 9780857098047. Available from: <http://linkinghub.elsevier.com/retrieve/pii/B9780857098047500029>
- [14] GINEBRA, M.P., T. TRAYKOVA and J.A. PLANELL. Calcium phosphate cements as bone drug delivery systems: A review: A review. *Journal of Controlled Release*. 2006, 113(2), 102-110. DOI: 10.1016/j.jconrel.2006.04.007. ISSN 01683659. Available from: <http://linkinghub.elsevier.com/retrieve/pii/S0168365906001775>
- [15] FERNÁNDEZ, E., M. P. GINEBRA, O. BERMÚDEZ, M. G. BOLTONG, F. C. M. DRIESSENS and J. A. PLANELL. Dimensional and thermal behaviour of calcium phosphate cements during setting compared to PMMA bone cements. *JOURNAL OF MATERIALS SCIENCE LETTERS*. 14. England: Chapman & Hall, 1995, 4/5. ISBN 0261-8028.
- [16] O'NEILL, R., H.O. MCCARTHY, E.B. MONTUFAR, M.-P. GINEBRA, D.I. WILSON, A. LENNON and N. DUNNE. Critical review: Injectability of calcium phosphate pastes and cements. *Acta Biomaterialia*. 2017, 50, 1-19. DOI: 10.1016/j.actbio.2016.11.019. ISSN 17427061. Available from: <http://linkinghub.elsevier.com/retrieve/pii/S1742706116306067>
- [17] BOHNER, M. and Xuân Nam. PHẠM. Calcium orthophosphates in medicine: from ceramics to calcium phosphate cements. *Injury*. 2000, 2000, 31, D37-D47. DOI: 10.1016/S0020-1383(00)80022-4. ISSN 00201383. Available from: <http://linkinghub.elsevier.com/retrieve/pii/S0020138300800224>

- [18] YUBAO, Li, Zhang XINGDONG and K. DE GROOT. Hydrolysis and phase transition of alpha-tricalcium phosphate. *Biomaterials*. 1997, 18(10), 737-741. DOI: 10.1016/S0142-9612(96)00203-7. ISSN 01429612. Available from: <http://linkinghub.elsevier.com/retrieve/pii/S0142961296002037>
- [19] ŞAHİN, Erdem and Dilhan M. KALYON. The rheological behavior of a fast-setting calcium phosphate bone cement and its dependence on deformation conditions. *Journal of Mechanical Behavior or Biomedical Materials*. 2017, 27(2017), 252-260. DOI: 10.1016/j.jmbbm.2017.05.017. ISBN 10.1016/j.jmbbm.2017.05.017. Available from: <http://linkinghub.elsevier.com/retrieve/pii/S1751616117302059>
- [20] DOROZHKIN, Sergey V. Calcium orthophosphates. *Biomater*. 2014, 1(2), 121-164. DOI: 10.4161/biom.18790. ISSN 2159-2535. Available from: <http://www.tandfonline.com/doi/abs/10.4161/biom.18790>
- [21] ELIAZ, Noam and Noah METOKI. Calcium Phosphate Bioceramics: A Review of Their History, Structure, Properties, Coating Technologies and Biomedical Applications. *Materials*. 2017, 10(4), 334-. DOI: 10.3390/ma10040334. ISSN 1996-1944. Available from: <http://www.mdpi.com/1996-1944/10/4/334>
- [22] CHEN, Shyuan-Yow, Shih-Fu OU, Nai-Cia TENG, Chun-Ming KUNG, Hsien-Lung TSAI, Kuo-Tien CHU and Keng-Liang OU. Phase transformation on bone cement: Monocalcium phosphate monohydrate into calcium-deficient hydroxyapatite during setting. *Ceramics International*. 2013, 39(3), D37-D47. DOI: 10.1016/j.ceramint.2012.08.097. ISSN 02728842. Available from: <http://linkinghub.elsevier.com/retrieve/pii/S0020138300800224>
- [23] LIU, Changsheng, Huifang SHAO, Feiyue CHEN and Haiyan ZHENG. Rheological properties of concentrated aqueous injectable calcium phosphate cement slurry. *BIOMATERIALS*. 2006, 2006(27), 5003-5013. DOI: 10.1016/j.biomaterials.2006.05.043. ISBN 10.1016/j.biomaterials.2006.05.043. Available from: <http://linkinghub.elsevier.com/retrieve/pii/S0142961206004947>
- [24] GINEBRA, Maria-Pau, José-Angel DELGADO, Ingela HARR, Amisel ALMIRALL, Sergio DEL VALLE and Josep A. PLANELL. Factors affecting the structure and properties of an injectable self-setting calcium phosphate foam. *Journal of Biomedical Materials Research Part A*. 2007, 80A(2), 351-361. DOI: 10.1002/jbm.a.30886. ISSN 15493296. Available from: <http://doi.wiley.com/10.1002/jbm.a.30886>
- [25] AN, Jie, Joop G. C. WOLKE, John A. JANSEN and Sander C. G. LEEUWENBURGH. Influence of polymeric additives on the cohesion and mechanical properties of calcium phosphate cements. *Journal of Materials Science: Materials in Medicine*. 2016, 27(3), -. DOI: 10.1007/s10856-016-5665-x. ISSN 0957-4530. Available from: <http://link.springer.com/10.1007/s10856-016-5665-x>

- [26] HUANGTADIER, S., L. GALEA, B. CHARBONNIER, G. BAROUD and M. BOHNER. Phase and size separations occurring during the injection of model pastes composed of β -tricalcium phosphate powder, glass beads and aqueous solutions. *Acta Biomaterialia*. 2014, 10(5), 2259-2268. DOI: 10.1016/j.actbio.2013.12.018. ISBN 10.1016/j.actbio.2013.12.018. Available from: <http://linkinghub.elsevier.com/retrieve/pii/S1742706113006144>
- [27] MIYAZAKI, K., T. HORIBE, J.M. ANTONUCCI, S. TAKAGI and L.C. CHOW. Polymeric calcium phosphate cements: setting reaction modifiers. *Dental Materials*. 1993, 9(1), 46-50. DOI: 10.1016/0109-5641(93)90105-Y. ISSN 01095641. Available from: <http://linkinghub.elsevier.com/retrieve/pii/010956419390105Y>
- [28] HESARAKI, Saeed, Shokoufeh BORHAN, Ali ZAMANIAN and Masoud HAFEZI-ARDAKANI. Rheological properties and injectability of β -Tricalcium phosphate-Hyaluronic acid/Polyethylene glycol composites used for the treatment vesicourethral reflux. *Advances in Biomedical Engineering Research*. 2013, 1(3), 40-44.
- [29] CHAMRADOVÁ, I., L. VOJTOVÁ, K. ČÁSTKOVÁ, P. DIVIŠ, M. PETEREK and J. JANČÁŘ. The effect of hydroxyapatite particle size on viscoelastic properties and calcium release from a thermosensitive triblock copolymer. *Colloid and Polymer Science*. 2017, 295(1), 107-115. DOI: 10.1007/s00396-016-3983-7. ISSN 0303-402X. Available from: <http://link.springer.com/10.1007/s00396-016-3983-7>
- [30] MAAZOUZ, Yassine, Edgar B. MONTUFAR, Julien MALBERT, Montserrat ESPANOL and Maria-Pau GINEBRA. Self-hardening and thermoresponsive alpha tricalcium phosphate/pluronic pastes. *Acta Biomaterialia*. 2017, 49, 563-574. DOI: 10.1016/j.actbio.2016.11.043. ISSN 17427061. Available from: <http://linkinghub.elsevier.com/retrieve/pii/S1742706116306407>
- [31] HUH, Hyun Wook, Linlin ZHAO and So Yeon KIM. Biomimetic organic/inorganic hybrid hydrogels based on hyaluronic acid and poloxamer. *Carbohydrate Polymers*. 2015, 126, 130-140. DOI: 10.1016/j.carbpol.2015.03.033. ISSN 01448617. Available from: <http://linkinghub.elsevier.com/retrieve/pii/S0144861715002465>
- [32] QIAO, Mingxi, Dawei CHEN, Xichen MA and Yanjun LIU. Injectable biodegradable temperature-responsive PLGA-PEG-PLGA copolymers: Synthesis and effect of copolymer composition on the drug release from the copolymer-based hydrogels. *International Journal of Pharmaceutics*. 2005, 294(1-2), 103-112. DOI: 10.1016/j.ijpharm.2005.01.017. ISSN 03785173. Available from: <http://linkinghub.elsevier.com/retrieve/pii/S0378517305000840>
- [33] Thermoreversible Gelation of PEG-PLGA-PEG Triblock Copolymer Aqueous Solutions. *Macromolecules*. 1999, 32(21), 7064-7069. DOI: 10.1021/ma9908999. ISSN 0024-9297. Available from: <http://pubs.acs.org/doi/abs/10.1021/ma9908999>

- [34] MICHLOVSKÁ, Lenka, Lucy VOJTOVÁ, Ludmila MRAVCOVÁ, Soňa HERMANOVÁ, Jiří KUČERÍK and Josef JANČÁŘ. Functionalization Conditions of PLGA-PEG-PLGA Copolymer with Itaconic Anhydride. *Macromolecular Symposia*. 2010, 295(1), 119-124. DOI: 10.1002/masy.200900071. ISSN 10221360. Available from: <http://doi.wiley.com/10.1002/masy.200900071>
- [35] LEE, Doo Sung, Myung Seob SHIM, Shung Wan KIM, Hyunjung LEE, Insun PARK and Tainhyun CHANG. Macromol. Rapid Commun. 2001, 22, 587–592
587 Novel Thermoreversible Gelation of Biodegradable PLGA-block-PEO-block-PLGA Triblock Copolymers in Aqueous Solution. *Macromolecular Rapid Communication*. 2001, 22(8), 587-592.
- [36] WANG, Xiupeng, Jiandong YE and Hai WANG. Effects of additives on the rheological properties and injectability of a calcium phosphate bone substitute material. *Journal of Biomedical Materials Research Part B: Applied Biomaterials*. 2006, 78B(2), 259-264. DOI: 10.1002/jbm.b.30481. ISSN 1552-4973. Available from: <http://doi.wiley.com/10.1002/jbm.b.30481>
- [37] WANG, Xiupeng, Ling CHEN, Hong XIANG and Jiandong YE. Influence of anti-washout agents on the rheological properties and injectability of a calcium phosphate cement. *Journal of Biomedical Materials Research Part B: Applied Biomaterials*. 2007, 81B(2), 410-418. DOI: 10.1002/jbm.b.30678. ISSN 15524973. Available from: <http://doi.wiley.com/10.1002/jbm.b.30678>
- [38] WALEROUX, L, Z HATIM, M FRÈCHE and J.L LACOUT. Effects of various adjuvants (lactic acid, glycerol, and chitosan) on the injectability of a calcium phosphate cement. *Bone*. 1999, 25(2), 31S-34S. DOI: 10.1016/S8756-3282(99)00130-1. ISSN 87563282. Available from: <http://linkinghub.elsevier.com/retrieve/pii/S8756328299001301>
- [39] HUANG, Shishu, Nuanyi LIANG, Yang HU, Xin ZHOU and Nouredine ABIDI. Polydopamine-Assisted Surface Modification for Bone Biosubstitutes. *BioMed Research International*. 2016, 2016, 1-9. DOI: 10.1155/2016/2389895. ISSN 2314-6133. Available from: <http://www.hindawi.com/journals/bmri/2016/2389895/>
- [40] LIU, Yanlan, Kelong AI and Lehui LU. Polydopamine and Its Derivative Materials: Synthesis and Promising Applications in Energy, Environmental, and Biomedical Fields. *Chemical Reviews*. 2014, 114(9), 5057-5115. DOI: 10.1021/cr400407a. ISSN 0009-2665. Available from: <http://pubs.acs.org/doi/10.1021/cr400407a>
- [41] Mussels' sticky secrets and energy-absorbing materials. In: *Science Learning Hub* [online]. The University of Waikato (New Zeland), 2013 [cit. 2018-03-25]. Available from: <https://www.sciencelearn.org.nz/resources/2191-mussels-sticky-secrets-and-energy-absorbing-materials>

- [42] BALL, Vincent. Determination of the extinction coefficient of “polydopamine” films obtained by using NaIO₄ as the oxidant. *Materials Chemistry and Physics*. 2017, **186**, 546-551. DOI: 10.1016/j.matchemphys.2016.11.035. ISSN 02540584. Available from: <http://linkinghub.elsevier.com/retrieve/pii/S0254058416308586>
- [43] FAN, Ka Wai, Justine J. ROBERTS, Penny J. MARTENS, Martina H. STENZEL and Anthony M. GRANVILLE. Copolymerization of an indazole ligand into the self-polymerization of dopamine for enhanced binding with metal ions. *Journal of Materials Chemistry B*. 2015, 3(37), 7457-7465. DOI: 10.1039/C5TB01150G. ISSN 2050-750X. Available from: <http://xlink.rsc.org/?DOI=C5TB01150G>
- [44] YANG, Kisuk, Jung Seung LEE, Jin KIM, et al. Polydopamine-mediated surface modification of scaffold materials for human neural stem cell engineering. *Biomaterials*. 2012, 33(29), 6952-6964. DOI: 10.1016/j.biomaterials.2012.06.067. ISSN 01429612. Available from: <http://linkinghub.elsevier.com/retrieve/pii/S014296121200717X>
- [45] KAO, Chia-Tze, Chi-Chang LIN, Yi-Wen CHEN, Chia-Hung YEH, Hsin-Yuan FANG and Ming-You SHIE. Poly(dopamine) coating of 3D printed poly(lactic acid) scaffolds for bone tissue engineering. *Materials Science and Engineering: C*. 2015, 56, 165-173. DOI: 10.1016/j.msec.2015.06.028. ISSN 09284931. Available from: <http://linkinghub.elsevier.com/retrieve/pii/S0928493115301624>
- [46] SUN, Xiaoming, Liying CHENG, Jingwen ZHAO, et al. BFGF-grafted electrospun fibrous scaffolds via poly(dopamine) for skin wound healing. *J. Mater. Chem. B*. 2014, 2(23), 3636-3645. DOI: 10.1039/C3TB21814G. ISSN 2050-750X. Available from: <http://xlink.rsc.org/?DOI=C3TB21814G>
- [47] SKALICKOVA, Sylvie, Vedran MILOSAVLJEVIC, Kristyna CIHALOVA, Pavel HORKY, Lukas RICHTER and Vojtech ADAM. Selenium nanoparticles as a nutritional supplement. *Nutrition*. 2017, **33**, 83-90. DOI: 10.1016/j.nut.2016.05.001. ISSN 08999007. Available from: <http://linkinghub.elsevier.com/retrieve/pii/S0899900716300727>
- [48] KODERA, Toshiaki, Hiroyuki TADA, Ayumi AKAZAWA, et al. Evaluation of the Use of Calcium Phosphate Cement for Aesthetic Neurosurgical Cranial Reconstruction. *World Neurosurgery*. 2018, 110, e296-e304. DOI: 10.1016/j.wneu.2017.10.153. ISSN 18788750. Available from: <http://linkinghub.elsevier.com/retrieve/pii/S1878875017318818>
- [49] HABRAKEN, Wouter, Pamela HABIBOVIC, Matthias EPPLE and Marc BOHNER. *Materials Today*. 2016, 19(2). DOI: 10.1016/j.mattod.2015.10.008. ISSN 13697021. Available from: <http://linkinghub.elsevier.com/retrieve/pii/S136970211500317X>

- [50] BOHNER, M., U. GBURECK and J.E. BARRALET. Technological issues for the development of more efficient calcium phosphate bone cements: A critical assessment. *Biomaterials*. 2005, 26(33), 6423-6429. DOI: 10.1016/j.biomaterials.2005.03.049. ISSN 01429612. Available from: <http://linkinghub.elsevier.com/retrieve/pii/S0142961205003844>
- [51] BARNES, Howard A. A HANDBOOK OF ELEMENTARY RHEOLOGY. University of Wales: The University of Wales Institute of Non-Newtonian Fluid, 2000. ISBN 0-9538032-0-1.
- [52] BARTOVSKÁ, Lidmila and Marie ŠIŠKOVÁ. *Fyzikální chemie povrchů a koloidních soustav*. Vyd. 5., přeprac. Praha: Vysoká škola chemicko-technologická, 2005. ISBN 80-708-0579-X.
- [53] MEWIS, Jan and Norman J. WAGNER. Thixotropy. *Advances in Colloid and Interface Science*. 2009, 147-148, 214-227. DOI: 10.1016/j.cis.2008.09.005. ISSN 00018686. Available from: <http://linkinghub.elsevier.com/retrieve/pii/S0001868608001735>
- [54] VERNON, Brent. *Injectable biomaterials: science and applications*. Philadelphia: Woodhead Pub., 2011. ISBN 978-1-84569-588-0.
- [55] LIU, Changsheng, LIU, Changsheng, Huifang SHAO, Feiyue CHEN and Haiyan ZHENG. Rheological properties of concentrated aqueous injectable calcium phosphate cement slurry. *Biomaterials*. 2006, 27(2006), 5003-5013. DOI: 10.1016/j.biomaterials.2006.05.043. ISBN 10.1016/j.biomaterials.2006.05.043. Available from: <http://linkinghub.elsevier.com/retrieve/pii/S0142961206004947>
- [56] Discovery HR-2. TA instruments [online]. [cit. 2018-03-21]. Available from: <http://www.tainstruments.com/dhr-2/>
- [57] TA INSTRUMENT. *Rheology Theory and Applications Course*. 2008. vyd. USA.
- [58] TA INSTRUMENT. *AR & ARES Rheometer Certified User Course ITheory*. 2006. vyd. USA.
- [59] MALKIN, Aleksandr Jakovlevič. *Rheology fundamentals*. Toronto-Scarborough: ChemTec Publishing, c1994. Fundamental topics in rheology. ISBN 978-189-5198-096.
- [60] SPERLING, L. H. *Introduction to physical polymer science*. 4th ed. Hoboken, N.J.: Wiley, c2006. ISBN 978-0-471-70606-9.
- [61] MICHLOVSKÁ, L., L. VOJTOVÁ, O. HUMPA, J. KUČERÍK, J. ŽÍDEK and J. JANČÁŘ. Hydrolytic stability of end-linked hydrogels from PLGA–PEG–PLGA macromonomers terminated by α,ω -itaconyl groups. *RSC Advances*. 2016, 6(20), 16808-16816. DOI: 10.1039/C5RA26222D. ISSN 2046-2069. Available from: <http://xlink.rsc.org/?DOI=C5RA26222D>

8 LIST OF TABLES

Tab. 1: CaP compounds and their major properties [13, 17, 20].	14
Tab. 2: Possible additives and their effects on CPC properties.	16
Tab. 3: Commercial calcium phosphate cements with their composition (when available) [50].	20
Tab. 4: Type of dynamic rheological testing methods [55].	28
Tab. 5: Summary of analysed samples, their composition and visual characteristics.	39

9 LIST OF FIGURES

Fig. 1: The hierarchical structure of lamellar bone from macro to nano scale [4].....	9
Fig. 2: Schema of bone cement application demonstrated on a humeral defect, (A) bone defect, (B) application of cement by injection, (C) remodeling and bone regeneration [8].	11
Fig. 3: Types of CPC. Schema of possible reactions and examples of precursors using for CPCs preparation [12].	12
Fig. 4: Schema of PLGA-PEG-PLGA triblock copolymer.	15
Fig. 5: Phase diagram of aqueous solution of PLGA-PEO-PLGA triblock copolymer.	15
Fig. 6: Mussel attached to the surface of a piece of brick by plaque fibers [41].	18
Fig. 7: The schema of DOPA polymerization reaction [40].	19
Fig. 8: Flow curves of time independent types of fluids.Reformed by [16].	24
Fig. 9: The course of setting of CPC. 1. processing period, 2. working period, 3. setting period, 4. final hardening period.	25
Fig. 10: Rotational rheometer (TA Instruments) [56].	25
Fig. 11: Types of geometry used for dynamic rheological analysis. Cone plate geometry and parallel plate geometry (from the left side) [58].	26
Fig. 12: Characterization of linear viscoelastic region (LVR), where modulus is independent of strain.	28
Fig. 13: Shear stress and shear rate relation of CPC [53].	29
Fig. 14: Calcium phosphate ceramics. MCP and α -TCP (from left side).	32
Fig. 15: 20% PLGA-PEG-PLGA copolymer solution.	32
Fig. 16: Rotational rheometer with solvent trap prepared for measurement.	34
Fig. 17: NMR spectrum of PLGA-PEG-PLGA triblock copolymer.	35
Fig. 18: Temperature dependence of 20% PLGA-PEG-PLGA aqueous solution, where 1 is sol-gel transition and 2 is the end of gelation.	36
Fig. 19: 20% PLGA-PEG-PLGA copolymer at gel phase.	36
Fig. 20: Hysteresis loop as a characterisation of PLGA-PEG-PLGA thixotropy.	37

Fig. 21: Viscosity versus shear rate of 20% PLGA-PEG-PLGA copolymer.....	37
Fig. 22: a) α -TCP partical size distribution. b) SEM micrograph of α -TCP.....	38
Fig. 23: a) MCP partical size distribution. b) SEM micrograph of MCP.	38
Fig. 24: a) particle size distribution and b) SEM micrograph of selenium nanoparticles.	39
Fig. 25: The relationship between shear stress and shear rate of samples W+C, ABA and ABA+C measured in rage of shear rates from 1 to 100 s ⁻¹	41
Fig. 26: The samples after steady state rheological measurement. The shear rate range from 1 to 100 % upward and from 100 to 1 % downward. From the left side: W+C, ABA+C.....	41
Fig. 27: Viscosity versus shear rate upward and downward flow paths at 23 °C. Samples: ABA, ABA+C, W+C.	42
Fig. 28: The relationship between shear stress and shear rate of samples ABA+C, ABA+C+D and ABA+C+D+I measured in rage of shear rates from 1 to 100 s ⁻¹	42
Fig. 29: Viscosity versus shear rate upward and downward flow paths at 23 °C. Samples: ABA+C, ABA+C+D, ABA+C+D+I.	43
Fig. 30: The relationship between shear stress and shear rate of samples ABA+C+SeNPs and ABA+C measured in rage of shear rates from 1 to 100 s ⁻¹	44
Fig. 31: Viscosity versus shear rate upward and downward flow paths at 23 °C. Samples: ABA+C, ABA+SeNPs+C.	44
Fig. 32: Calculated values of area of thixotropic hysteresis look for all studied modified pastes.	45
Fig. 33: Dynamic moduli of ABA+C sample at constant frequency (1 Hz), temperature 23 and 37 °C and changing strain at the range of 0.001-500 %.....	46
Fig. 34: Dynamic moduli of ABA+C sample at constant strain (0.01 %), temperature 23 and 37 °C and changing frequency at the range of 0.16-16 Hz.	47
Fig. 35: The relationship between complex viscosity and applied frequency range 0.16-16 Hz.....	47
Fig. 36: Time sweep response of G', G'' and η^* of ABA+C at 37 °C. Parameters of measurement: frequency 1 Hz, strain 0.01 %.	48
Fig. 37: Time sweep response of G' of ABA+C, ABA+C+D and ABA+C+D+I at 23 °C. Parameters of measurement: frequency 1 Hz, strain 0.01 %.....	49

Fig. 38: Time sweep response of G' of ABA+C, ABA+C+D and ABA+C+D+I at 37 °C. Parameters of measurement: frequency 1 Hz, strain 0.01 %.	49
Fig. 39: Time sweep response of G' of ABA+C, ABA+SeNPs+C at 23 °C. Parameters of measurement: frequency 1 Hz, strain 0.01 %.	50
Fig. 40: Time sweep response of G' and of ABA+C, ABA+SeNPs+C at 37 °C. Parameters of measurement: frequency 1 Hz, strain 0.01 %.	51

10 LIST OF ABBREVIATIONS

ABA	PLGA-PEG-PLGA
ACP	Amorphous calcium phosphate
BTE	Bone tissue engineering
C	Powder phase composed of MCP and α -TCP
CA	Citric acid
CaP	Calcium orthophosphates
CDCl ₃	Deuterated chloroform
CDHA	Calcium-deficient hydroxyapatite
CMC	Sodium Carboxymethyl Cellulose
CPC	Calcium phosphate cement
D	Dopamine
DCP	Dicalcium phosphate
DCPD	Dicalcium phosphate dihydrate
DHI	5,6-dihydroxyindole
DHP	Disodium hydrogen phosphate
DLS	Dynamic light scattering
DOPA	Dopamine
ECM	Extracellular matrix
GA	Glycolic acid
GPC	Gel permeation chromatography
HA	Hydroxyapatite
HABS	Hyaluronan-bisphosphate
HAc	Hyaluronic acid
I	Sodium Iodate
L/P	Liquid-powder ratio

LA	Lactic acid
LVR	Linear viscoelastic region
MCP	Monocalcium phosphate
MCPM	Monocalcium phosphate monohydrate
Mefp	"Mussel foot" proteins
nf	Not found
NMR	Nuclear magnetic resonance
OCP	Octacalcium phosphate
PCA	Polycarboxylic acid
PDI	Polydispersity index
PEG	Polyethyleneglycol
PEO	Poly(ethylene oxide)
PHA	Precipitated hydroxyapatite
PLA	Polylactic acid
PLGA-PEG-PLGA	Poly(D,L-lactic acid-co-glycolic acid)-b-poly(ethylene glycol)-b-poly(D,L-lactic acid-co-glycolic acid) triblock copolymer
SEM	Scanning electron microscopy
SeNPs	Selenium nanoparticles
TMS	Tetramethylsilane
TRIS	Tris(hydroxymethyl)aminoethane
TTCP	Tetracalcium phosphate
W	Distilled water
α -TCP	α -Tricalcium phosphate
β -TCP	β -Tricalcium phosphate

11 LIST OF SYMBOLS

τ, τ', τ''	Shear stress
G^*	Complex modulus
G'	Storage modulus
G''	Loss modulus
K	Flow consistency index
n	Flow behavior index
t	Time
T	Temperature
γ	Shear rate
$\tan \delta$	Loss tangent
δ	Shift
η	Viscosity
η^*	Complex viscosity
ω	Angular frequency